Coastal Engineering 168 (2021) 103939

Contents lists available at ScienceDirect

Coastal Engineering

journal homepage: www.elsevier.com/locate/coastaleng

Using a two-step framework for the investigation of storm impacted beach/dune erosion

Pushpa Dissanayake [a,*], Jennifer Brown [b], Philipp Sibbertsen [c], Christian Winter [a]

[a] Coastal Geology and Sedimentology, Institute of Geosciences, Otto-Hahn-Platz 1, 24118, Kiel, Germany
[b] National Oceanographic Centre, Joseph Proudman Building, 6 Brownlow Street, Liverpool, L3 5DA, UK
[c] Institute of Statistics, Leibniz University Hannover, Königsworther Platz 1, 30167, Hannover, Germany

ARTICLE INFO

Keywords:
Classification of storm events
Statistical analysis
Numerical modelling
Beach/dune erosion
Inter-storm recovery
Coastal hazard
XBeach
Formby point
Sefton coast

ABSTRACT

Long-term coastal management of beach/dune systems requires the definition and assessment of storm events. This study presents a framework using statistical analyses and numerical modelling (XBeach) to characterize storm events and investigate their impact on beach/dune erosion. The method is developed using exemplary data from Formby Point on the Sefton coast (UK), which has a complex beach morphology and frontal dunes. Relevant storm events are classified by a versatile univariate response function taking into account both nearshore water levels and offshore significant wave heights (*Hs*). It is shown that compared to the established storm classification ($Hs \geq 2.5$ m) 35% more storm events that are relevant for beach/dune erosion are identified. Also the events exceed critical conditions for longer durations, and cause greater erosion impact (12%) along the beach/dune profile. The proposed classification of storm events thus captures relevant events for the storm erosion and can inform coastal management strategies. This framework is widely applicable to other beach/dune systems.

1. Introduction

Beach/dune systems are common coastal landforms of high environmental and socio-economic value, and provide safety for the hinterland areas from coastal inundation (Kalligeris et al., 2020; Karunarathna et al., 2018; Hanley et al., 2014; Harley and Ciavola, 2013). Storm erosion of beach/dune systems poses a major challenge for sustainable coastal management but there is no unique approach to assess the stability and risk of erosion. However, the assessment of the beach/dune systems is becoming increasingly important worldwide to implement suitable mitigation strategies able to withstand future sea level rise and climate change scenarios (Vousdoukas et al., 2020; Masselink et al., 2016). Storm events play a prominent role in the assessment of coastal stability thus any assessment combines two steps. First, the occurrence of storm events needs to be accurately identified, which involves a storm classification, and then the erosion risk needs to be analysed using a reliable method. Identifying storm events from time series of environmental data (e.g. wave height, water level) provides the variability of storm events, which is the primary information for any subsequent analysis of storm impacts.

There are different classifications, which are commonly used to identify the occurrence of storm events. Peak tidal values within a window-size of three days were used to classify the storm occurrence at Egmond aan Zee, the Netherlands (Baart, 2013). Garnier et al. (2018) also used this approach to identify the historical storm events at different sites in Europe. This approach of peak tidal values, however, estimates very extreme events only (e.g. 1953 storm event in North Sea, Spencer et al., 2015). For Italian coasts, Bertotti et al. (1996) defined a storm event as the offshore significant wave height (*Hs*) is higher than 2 m and the inter-storm period is higher than 24 h, while Corsini et al. (2004) suggested that *Hs* should be higher than 1 m for at least 12 h in storm events. Armaroli et al. (2012) investigated the resilience of the Adriatic coast considering the dune erosion for different return levels of wave heights. They defined storm events as sea states of which *Hs* remains higher than 1.5 m for a period of more than 6 h. For the Narrabeen coast (Australia), Callaghan et al. (2008) estimated the occurrence of storm events based on a threshold *Hs* ($\geq$3 m). The 1% exceedance value of *Hs* was used to define storm events at the SW coast of UK (Masselink et al., 2016). The Channel Coastal Observatory (www.channelcoast.org) has defined a range of *Hs* thresholds to estimate the occurrence of storm events for the UK coasts based on the local wave heights (e.g. Sefton coast: $Hs \geq 2.5$ m). However, in macro tidal regimes the tidal cycle plays

* Corresponding author.
E-mail addresses: pushpa.dissanayake@ifg.uni-kiel.de (P. Dissanayake), jebro@pol.ac.uk (J. Brown), sibbertsen@statistik.uni-hannover.de (P. Sibbertsen), christian.winter@ifg.uni-kiel.de (C. Winter).

https://doi.org/10.1016/j.coastaleng.2021.103939
Received 21 June 2019; Received in revised form 26 May 2020; Accepted 9 June 2021
Available online 12 June 2021

a key role in mediating when waves can have an impact on a beach/dune system. For example, along the Sefton coast low waves can also increase the erosion of a beach/dune system, if the water level is sufficiently high (Pye and Blott, 2016). Pye and Blott (2006) determined severe storm events on the Suffolk coast (UK) considering the tidal anomalies (*TA* = Observed tide -Astronomical tide), *TA* > 1 m. Both *Hs* and *TA* have also been employed together to define the storm occurrence, but with two separate thresholds (Quartel et al., 2007). Li et al. (2014) used an arbitrary threshold for *Hs* with the *TA* threshold from Quartel et al. (2007) for their statistical analysis of storm events. All these examples indicate that a classification of storm events is generic, whereas thresholds are site-specific depending on the local hydrodynamics. There is no clear criterion present to transfer one classification to another coastal system or to combine wave and water level classifications in macrotidal regimes where both parameters are important for a storm to have an impact. Obviously, the occurrence of a high *Hs* is a common choice to identify storm events. However, during low water at a macrotidal location the waves will have no impact on the beach/dune system, while during high water levels, erosion at beach/dune systems may occur under low wave heights, increasing markedly during high water levels and high wave heights (Dissanayake et al., 2019a). Being able to capture this interaction is of prime importance to classify impactful storm events.

Different statistical approaches have been suggested to estimate storm events by considering the joint occurrence of high water levels and wave heights. Li et al. (2014) classified a storm event when both *Hs* and *TA* exceed the respective thresholds. A two-step analysis was proposed for a univariate case (e.g. *Hs*) in Bernardara et al. (2014). In the first step, independent events are identified using a threshold. In the second step, the selected events are fit with an extreme value probability distribution to estimate an optimised value, which is then used to identify the final independent storm events. This univariate approach was extended to bivariate analysis using a univariate response function of temporal water levels and wave heights for the investigation of coastal flooding (Mazas and Hamm, 2017). They first transformed offshore measured *Hs* to nearshore values using analytical formulas (Goda, 2010) and incorporated an analysis with the nearshore water levels. These analytical formulas of wave transformation are pertinent under the assumption of alongshore uniformity of a coastal system. Therefore, we employ a bivariate analysis considering the joint occurrence of offshore measured *Hs* and nearshore water levels to develop a classification of storm events at the Sefton coast (UK), which has a complex nearshore morphology.

To estimate the erosion of beach/dune systems during storm impact, the process-based numerical model XBeach has successfully been used in numerous case studies. XBeach (Roelvink et al., 2009) is an open-source coastal morphodynamic model, which was initially developed to simulate the hurricane impact at sandy barrier islands, and the model skills are being continuously improved (e.g. Roelvink et al., 2018; McCall et al., 2015). Using XBeach, Van Ormondt et al. (2020) investigated the evolution of the wilderness breach (Fire Island, New York). Results concluded that large sediment import into the bay during breaching does not affect the littoral transport and hence no increased downdrift erosion. Harley and Ciavola (2013) used XBeach to investigate the coastal inundation risk by the beach/dune erosion at the Emilia-Romagna coast. Results showed the vulnerable areas along the coast providing the required understanding to improve the management of the dunes. Smallegan et al. (2016) simulated the impacts of a buried sea wall on the resilience of a beach/dune system during Hurricane Sandy. A comparison of the hydrodynamics and morphodynamics influencing the dune response between the laboratory experiments and the XBeach models was carried out in Berard et al. (2017). Results indicated the sensitivity of the dune erosion to the parameterization of XBeach (*dryslp*: dry slope, *wetslp*: wet slope and *eps*: threshold depth for wet cells). Storm erosion on the Sefton coast was simulated using 2DH (area-model) and 1D (profile-model) approaches in Dissanayake et al. (2014; 2015c). The 2DH modelling (Dissanayake et al., 2014) produced good agreements of the profile erosion with the measured data (*Brier--Skill-Score*>0.8 and R^2>0.5) and showed different vulnerability to storm impacts along the coast. The 1D modelling (Dissanayake et al., 2015c) presented the impacts of storm clustering by increasing the susceptibility to the beach/dune erosion. These studies support the credibility of XBeach and highlight the need to derive a statistical framework to generate the model boundary forcing of storm events in order to analyse the storm erosion risks.

The objective of this study is to develop a classification of storm events considering the joint occurrence of high water levels and high wave heights, and to analyse the storm impact on a beach/dune system. Our hypothesis is that the existing storm definition for the Sefton coast (*Hs* ≥ 2.5 m) may not capture all relevant storm events that are able to erode the beach/dune system. For the statistical analysis, we use offshore *Hs* and nearshore water levels. 1D simulations using XBeach are carried out to investigate the storm erosion. A proposed two-step framework is developed based on the Sefton coast and generalized to other beach/dune systems using the local information, to identify the occurrence of storm events and to estimate the erosion risk.

The structure of this paper is as follows. Section 2 describes study area and field data, and the approach is introduced in section 3. Results are included in section 4, and the discussion of the results is in section 5. Conclusions of this study are given in section 6.

2. Study area and field data

2.1. Study area

The Sefton coast is located in the Liverpool Bay at the northwest coast of the UK (Fig. 1a). The beach/dune system of the Sefton coast represents about 20% of the UK's entire dune systems and extends about 4 km landward with the maximum dune height reaching about 20 m (Souza et al., 2013; Edmondson, 2010). The Sefton coast has a convex shape spanning about 36 km from the Mersey estuary (to the south) to the Ribble estuary (to the north). The apex of this coast is at Formby Point (Fig. 1b), which acts as a sediment divergence zone with eroding beaches at Formby Point and accreting beaches to the north and the south. Esteves et al. (2009) estimated that the annual dune retreat at Formby Point was about 5 m during the period from 2001 to 2008, affecting the morphological evolution of the entire Sefton coast.

The inter-tidal area of the Sefton coast is characterized by a shore-parallel ridge-runnel pattern (Fig. 1c), which is from 0.5 m to 1.0 m in height between a crest and a trough, and from 150 m to 500 m in distance between crests and troughs, with a very mild slope of about 1:100 (Plater and Grenville, 2010). Of the measured profile on September 10, 2013 (blue-line in Fig. 1d), the ridge-runnel pattern indicates a height of about 0.5 m and a distance of <100 m within the upper beach. The Sefton dune foot (+4.8 m ODN: Ordinary Datum Newlyn ~ MSL) is located just above the mean spring high water level and the dune profile has steep gradients, particularly around Formby Point (Dissanayake et al., 2015c). It should be noted that water level and bed elevations are hereon referred to ODN. Episodic dune erosion at Formby Point occurs by soaking and the direct wave impacts at the dune toe, when the water level exceeds about 5.2 m (Parker, 1975). A recent example of such storm events is found in the 2013/2014 winter. During the first event of this period, the peak storm wave (~4.5 m) coincided with a water level of 6.2 m (Pye and Blott, 2016) which resulted in a dune retreat of about 4 m. At low water levels, the dune toe is impacted by wave run-up rather than soaking. The potential of erosion increases with the height of tidal anomalies (*TA*) and high wave energy (Halcrow, 2009). The sediment properties of this coast are determined by the tide dominated net onshore transport and the inflow of the adjacent estuaries. Bed sediment composition of the Sefton coast may be described by a median grain size (D_{50}) in the range of 0.1–0.3 mm (Pye and Blott, 2008).

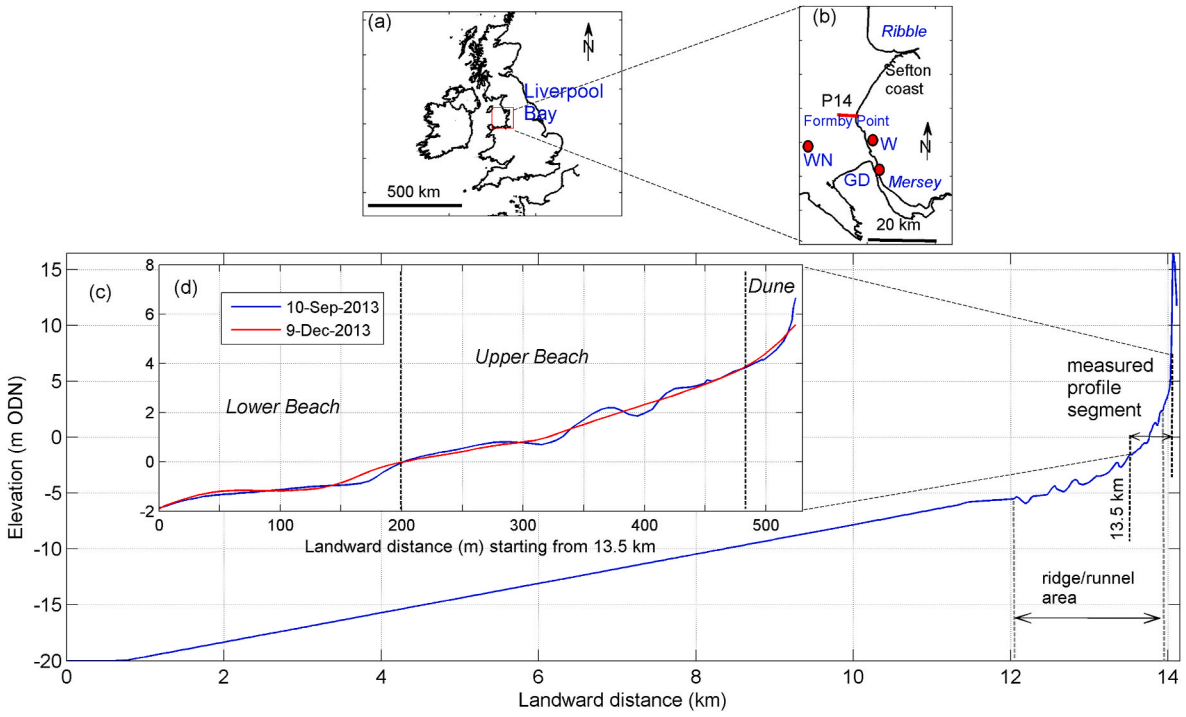

Fig. 1. Location of the Liverpool Bay and the Sefton coast (a), selected profile (P14) at Formby Point, Tides at Gladstone Dock (GD), Waves at the WaveNet buoy (WN) and Winds (W) at the Crosby station (b), 1D XBeach domain (c), and the profile segments for the analysis with the pre- and the post-storm measured profiles (d).

2.2. Field data

Marine forcing from tides and waves, and winds continuously shape this beach/dune system. These data from 2005 to 2018 are used for the statistical analysis. Liverpool Bay has an alongshore propagating semi-diurnal tide with a mean spring tidal range increasing up to about 8.2 m (Palmer, 2010). Large *TA*s generally occur during the rising tide (Brown et al., 2010b) and the maximum *TA* recorded at high water tide in the Liverpool Bay has been reported to about 2 m at Gladstone Dock (GD in Fig. 1b) on January 03, 1976 (Pye and Blott, 2016). We use the recorded water levels and the estimated *TA*s at GD by the National Tidal and Sea Level Facility (www.ntslf.org) from the British Oceanographic Data Centre (www.bodc.ac.uk). The *TA* data (blue-line) is shown in Fig. 2. Vertical bars of this figure indicate the selected storm years for the analysis considering the periods from the end-summer to the begin-summer of the adjacent year in order to avoid of splitting winter storm events. High *TA*s have occurred in the winter months of each year and the values higher than 2 m correspond to low water tide. The maximum *TA* of about 2.5 m has occurred on November 15, 2015 during the rising tide at −1 m.

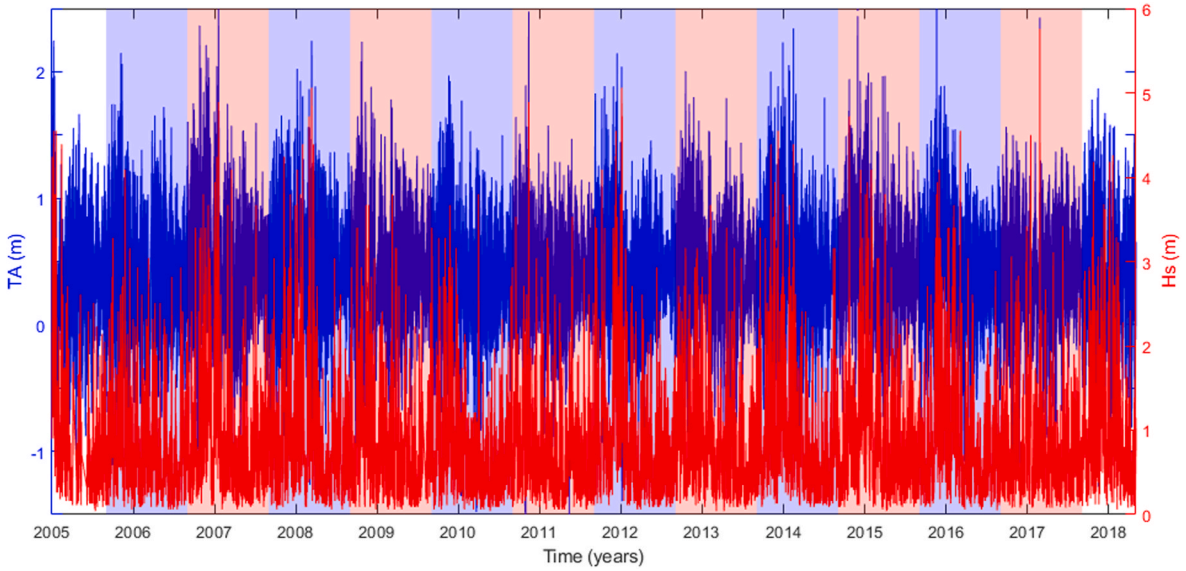

Fig. 2. Estimated tidal anomalies (TA: blue-line) from the measured water levels at Liverpool Gladstone Dock (GD in Fig. 1b), and the measured significant wave heights (Hs: red-line) at the WaveNet location (WN in Fig. 1b). Vertical columns indicate from end-summer to begin-summer years. (For interpretation of the references to colour in this figure legend, the reader is referred to the Web version of this article.)

Wave data in Liverpool Bay is available at the WaveNet buoy from the Centre for Environment, Fisheries and Aquaculture Science (www.wavenet.cefas.co.uk), which is located at 22 m water depth (WN in Fig. 1b). These data have a temporal resolution of 0.5 h. Long-term wave characteristics show that the mean annual *Hs* is about 0.5 m while the extremes reach about 6 m (Brown et al., 2010a). The largest wave conditions are associated with west to north-west winds, where the longest fetch exists (Wolf et al., 2011). Variation of *Hs* within the analysis period shows that higher wave heights have also occurred during the winter months (red-line in Fig. 2), coinciding with the periods of higher *TA*s.

Wind data is used from a land-based station at Crosby (W in Fig. 1b) available from the Centre for Environmental Data Analysis (www.ceda.ac.uk) archives. The Crosby station is the nearest wind station to Formby Point. The wind data has a 1 h temporal resolution and the wind direction has been recorded to the nearest 10°. Average wind speed during the analysis period is about 11.5 m/s (maximum ~ 50 m/s) and the main wind direction is from S to W, while high winds approach from W to N.

Beach/dune profiles are biannually (spring and autumn) monitored at predefined locations along the Sefton coast by the local council (Sefton Metropolitan Borough Council). In 2013, an additional measuring campaign has been undertaken in winter. These profiles, however, do not represent the pre- and post-storm status of individual storm events. Therefore, we select the measured profiles in the autumn (10.09) and the winter (09.12) 2013 (see Fig. 1d) to perform numerical simulations using XBeach by forcing with the derived storm events. Positions of the dune toe have been surveyed using kinematic DGPS along the coast. We select 5 dune toe surveys (18.09, 24.09, 04.10, 29.11 and December 13, 2013), which represent the profile measurement period. The dune toe surveys have a spatial resolution of about 10 m. The nearshore bathymetry of the Sefton coast is obtained from the POLCOMS model, which has about 50 m spatial resolution within the nearshore area (Brown et al., 2010a).

3. Approach

Our approach is a two-step framework to investigate storm erosion of a beach/dune system. First, a classification of storm events (CASE) is developed using multivariate analysis in statistical methods to identify the storm occurrence. Numerical modelling is thereafter carried out to analyse the erosion of a beach/dune profile forced with the derived storm events.

3.1. Statistical analysis

There are different methods of multivariate analysis to identify an extreme event described by, 1) several parameters (e.g., wave height, peak wave period, peak wave direction: Callaghan et al., 2008), 2) several elementary processes (e.g., a sea level made of mean sea level, astronomical tide, wave setup etc.: Haigh et al., 2010), 3) joint occurrence of parameters (e.g., wave height, sea level: Li et al., 2014). We use the last method with the two parameters *Hs* and tidal anomaly (*TA*), which have been already used in several studies to identify storm events impacting the beach/dune systems (Pye and Blott, 2006; Masselink et al., 2016; Li et al., 2014; Quartel et al., 2007). Variations of *Hs* at WN and nearshore *TA* at GD (see Fig. 1b) are used to develop a storm threshold by statistical methods. A single threshold for both parameters is derived using a combined approach of the univariate function (Bernardara et al., 2014) and the bivariate analysis (Mazas and Hamm, 2017). We define our combined storm impact parameter following the bivariate analysis as in Eq. (1).

$$X(t) = Hs(t) + TA(t) \tag{1}$$

where t varies from 2005 to 2018.

The variable X is a compound variable from two others and therefore its probability distribution is derived as the convolution of the two marginal distributions from *TA* and *Hs*. We interest in the probability for exceedances of a threshold X. This exceedance probability might be dominated by one of the variables or it may be decreased by one variable, if both are very distinct in size or variability and behavior. However, the increase of *TA* and *Hs* occurs by the same extreme environmental forcing (Haigh et al., 2016; Pye and Blott, 2016), and they perceive a positive correlation. This makes sure that both variables behave similar by showing simultaneous upwards and downwards movements. As mentioned in 2.2, the mean annual *Hs* is about 0.5 m, while reaching about 6 m during extremes (Brown et al., 2010b). Positive *TA* is often less than 0.5 m and increases ~2.5 m during extremes (Brown et al., 2010a). Small negative *TA* (−0.5 – 0 m) in the Liverpool Bay can occur based on the wind approach and the tidal phase (Dissanayake et al., 2014). Both parameters have the same order of magnitude, therefore they can be used with the similar weighting in the sampling process (Eq. (1)). Same X can occur from small *TA* and *Hs*, which result in low X values. For the analysis of storm threshold, the maximum X of each event is used. Therefore, these low X values from small *TA* and *Hs* do not affect the storm threshold selection. Both findings, the similar magnitude of both variables and the positive correlation, make sure that the exceedance probability of the compound variable is not biased by only one of the two variables in either direction.

The statistical analysis is carried out according to the methodology proposed by Bernardara et al. (2014). Independent sets of storm events are derived using percentile values of X. We herein define several sample sets for a range of percentile values from 90% to 99%. Minimum storm durations of these events are set to be more than 1 h, and the spacing from the end of a storm event to the beginning of the subsequent event is set at least 12 h (Dissanayake et al., 2015c). Independency of the storm occurrence is further analysed by fitting the sample sets of storm events with the *Poisson* distribution (Haight, 1967). The probability function of the *Poisson* distribution follows Eq. (2).

$$P(y) = e^{-\lambda}\frac{\lambda^y}{y!} \tag{2}$$

where, λ: average number of storm events per year from 2005 to 2018 and y: the occurrence of storm events in each year.

The *Poisson* distribution describes the probability of occurrence of a given number of events within a fixed interval of time, if the events occur with an average rate and independency. When the number of event occurrences follows a *Poisson* distribution, they claim to be independent events (Bernardara et al., 2011; Callaghan et al., 2008). The goodness of the fit between the *Poisson* distribution (E) and the measured data (M) is estimated using the χ^2 test (Bernardara et al., 2011) as in Eq. (3).

$$\chi^2 = \sum_{i=1}^{n}\frac{(M_i - E_i)^2}{E_i} \tag{3}$$

The optimised threshold for the proposed CASE is selected by comparing the occurrence of the maximum value of X (Eq. (1)) during each storm event with an extreme value probability distribution. We hereby use the *Generalized Pareto Distribution* (*GPD*) for the statistical optimisation. The cumulative distribution function of the *GPD* (Bernardara et al., 2014) is given by Eq. (4).

$$F(x) = 1 - \left[1 + k\left(\frac{x-\mu}{\sigma}\right)\right]^{-\frac{1}{k}} \tag{4}$$

where, k: shape parameter, σ: scale parameter and μ: location parameter, x: maximum X (Eq. (1)) during each storm event.

The location parameter (μ) is generally set to zero (Bernardara et al., 2014; Pickland, 1975). Then, both shape (k) and scale (σ) parameters describe the behavior of the *GPD*. For the selected sample sets of storm events, these two parameters are separately estimated using the method

of L-moments (Šimková, T., 2017; Hosking and Wallis, 1997). The *GPD* has the characteristics that k and the modified scale parameter ($\sigma^* = \sigma - ku$, u: the percentile value of X) will remain constant when the threshold increases (Bernardara et al., 2014; Jane et al., 2016). This in turn indicates that the selection of the *GPD* parameters is independent from the threshold limits. We use this criterion ('stability domain') to identify the optimised value of u enabling to develop the CASE for the Sefton coast.

The following statistical parameters are employed to compare the agreement between the theoretical *GPD* and the sample storm events. The *variance* (s^2) measures the squared deviation from the mean value of a sample set. The lower the variance the lower the spread of data. x is the maximum value of X from the sample storm events, y is the corresponding value from the *GPD*. $\bar{x}$ and $\bar{y}$ indicate mean values and n is the number of storm events (Eqs. (5) and (6)).

$$s^2_{sample} = \frac{\sum_{i=1}^{n}(x_i - \bar{x})^2}{n} \tag{5}$$

$$s^2_{GPD} = \frac{\sum_{i=1}^{n}(y_i - \bar{y})^2}{n} \tag{6}$$

The *bias* indicates tendency of the estimator to over- or under-predict the sample values. A good estimator provides lower *bias* (Eq. (7)).

$$Bias = \frac{\sum_{i=1}^{n}(x_i - y_i)}{n} \tag{7}$$

The Root-Mean-Square-Error (*RMSE*) indicates the standard deviation between the sample events and the *GPD* values (Eq. (8)). Lower *RMSE*s imply the better agreements.

$$RMSE = \sqrt{\frac{\sum_{i=1}^{n}(x_i - y_i)^2}{n}} \tag{8}$$

The coefficient of determination (R^2) is defined as the squared value of the coefficient of correlation (Krause et al., 2005), which quantifies the fraction of the variance of the sample events that is explained by the *GPD* (Eq. (9)).

$$R^2 = \left[\frac{\sum_{i=1}^{n}(x_i - \bar{x})(y_i - \bar{y})}{\sqrt{(x_i - \bar{x})^2 (y_i - \bar{y})^2}}\right]^2 \tag{9}$$

3.2. Numerical modelling

3.2.1. XBeach

XBeach is a 2DH coastal morphodynamic modelling system (Roelvink et al., 2009, 2018) for the estimation of dune erosion within four regimes: swash, collision, overwash and inundation as described by Sallenger (2000). In the swash-regime, the nearshore hydrodynamics are resolved by employing a 2DH description of wave groups and infragravity motions (Roelvink et al., 2009). Wave group forcing, which drives the infragravity motion and longshore and cross-shore currents, is derived from a time varying wave action balance equation. In the collision regime, sediment transport from the dry dune to the wet swash is estimated with an avalanching model using a critical dry slope and a critical wet slope. Sediment transport can be computed using the Soulsby-Van Rijn (Soulsby, 1997) and the Van Thiel-Van Rijn (Van Rijn, 2007) formulations. During swash and collision regimes, XBeach calculates offshore sediment transport by return flow and rip-current. This facilitates progressive erosion by removing sediment from the slumped dune face. In the overwash regime, XBeach calculates the landward sediment transport by the onshore flux of water, which is driven by the wave group forcing, and that results in depositing dune sand landward as overwash fans. In the inundation regime, dune breaching occurs due to the formation of a channel cutting through the dunes. The dune breaching is based on the sediment transport induced by the dynamic channel flow and the avalanching triggered by bank erosion.

This study uses XBeach version 1.23.5387 with the surf-beat mode, which includes wave-driven currents (alongshore current, rip currents), long (infragravity) waves, and runup and rundown of long waves (swash). The surf-beat mode is relevant for the swash-zone processes and fully valid for the dissipative beaches (e.g. Sefton coast). For the bed sediment composition, we use an average sand fraction with D_{50} of 0.2 mm (Pye and Blott, 2008). XBeach can speed up morphological changes using the *morfac* approach (Roelvink, 2006). However, real-time morphodynamic evolution during storm impacts is here simulated using no upscaling (*morfac* = 1).

3.2.2. Model domain

We use the calibrated 1D model domain presented in Dissanayake et al. (2015c). This beach/dune profile is located on Formby Point (see Fig. 1b) at the most exposed section of the Sefton beach/dune system. Previous studies using a 1D approach have shown high skills in simulating storm impacts at Formby Point, which experiences marginal alongshore transport (Dissanayake et al., 2015a, 2015c; Esteves et al., 2012; Pye and Blott, 2008). Furthermore, cross-shore transport dominates over alongshore transport during storm impacts, and thus 1D modelling has successfully been used to investigate storm impacted beach/dune erosion in straight (e.g. Kalligeris et al., 2020; Dissanayake et al., 2019b) and curved (Callaghan et al., 2013; Pender and Karunarathna, 2013) coastal systems. The cross-shore profile is defined from the dune crest to the −1.8 m contour using the measured profile on September 10, 2013 (i.e. the initial profile during the selected simulation period). The profile elevation from −2 to −8 m is estimated using the previous profile survey data (Esteves et al., 2012). Seaward constant bed slope of 1:500 is thereafter applied from −8 to −20 m contour based on the bathymetry of the POLCOMS model (Brown et al., 2010a). At the offshore boundary wave data can be accurately imposed from the point of observation (i.e. WN in Fig. 1b). A high grid resolution (minimum ~1 m) is applied at the beach/dune area to accurately represent the bed topography. Offshore a low resolution (maximum ~50 m) is used to ensure efficient computation times are achieved. Calibrated model parameters using the measured profile data for the XBeach simulations are shown in Table 1.

Erosion along the profile is analysed within three segments, which are defined based on the water level excursion. The threshold water level required at Formby Point for the onset of dune erosion due to wave runup/setup and wave under cutting is 3.9 m, while the recession of dune cliffs occurs by direct wave impacts and soaking when the water level rises more than 5.2 m (Pye and Blott, 2016). Of the measured initial and final profiles at Formby Point, both span from the 6.5 m contour on the dunes to the −1.8 m contour on the beach. For the analysis of the beach/dune erosion, we therefore define three segments along the profile (Fig. 1d) and) Lower Beach (from −1.8 to 0 m), 2) Upper Beach (from 0 to 3.9 m) and 3) Dunes (above 3.9 m). It should be noted that the lower beach includes partly the inter-tidal area below 0 m due to the limited length of the measured profiles.

Table 1
Calibrated model parameters for the XBeach simulations (*cf.* Dissanayake et al., 2015c).

Decription	Parameter	Calibrated Value
Chézy coefficient	*C*	57
Sediment transport formula	*form*	2 (Van Thiesel - Van Rijn)
Maximum shield value for overwash/sheet flow condition	*smax*	0.8
Additional shear dispersion factor to create advective mixing	*nuhv*	1
Threshold depth for drying and flooding	*eps*	0.005
Calibration factor for wave asymmetry transport	*facua*	0
Avalanching occurs when defined slope exceeded	*wetslp*	0.3

3.2.3. Simulations

Model simulations are carried out for the derived storm events using the proposed (u) and the established (H) CASEs. The simulation period spans from 10.09 to December 09, 2013 based on the availability of measured profiles (see Fig. 1d). For the model simulations, we employ the profile of 10.09 as the pre- and that of 09.12 as the post-storm profile. Within the simulation period, several storm events have occurred and there are calm periods between adjacent events (see Table 5). Thus, possible (partly) beach recovery must be assumed (Pender and Karunarathna, 2013). As the model is not expected to simulate the recovery of the beach/dune system with high accuracy (Bart, 2017), two end member scenarios are defined (Table 2). In scenario 1, we assume, the beach/dune profile is fully recovered (FR) from the impacts of the previous event, when the subsequent event occurs (i.e. each simulation of the storm events has the same initial profile). In scenario 2, the profile does not recover (NR) from the impacts of the previous event, when the subsequent storm event occurs. The final simulated profile of the previous event is then used as the initial profile for the simulation of the subsequent event. These two scenarios are therefore expected bounding the observed beach response, where partial to full recovery could have occurred between events.

For the comparison of profile evolution between the measured data and the simulated results, we use *RMSE* (x: bed levels of the measured profile and y: bed levels of the simulated profile in Eq. (8)) and *Brier-Skill-Score* (*BSS* in Eq. (10)) following Van Rijn et al. (2003).

$$BSS = 1 - \frac{< \left(z_{measured\ final} - z_{simulated\ final}\right)^2 >}{< \left(z_{measured\ initial} - z_{measured\ final}\right)^2 >} \tag{10}$$

where, z: bed level along the beach/dune profile. The *BSS* is categorized for the model skill as, 0.3–0.0: Poor, 0.6–0.3: Reasonable/Fair, 0.8–0.6: Good and 1.0–0.8: Excellent.

4. Results

4.1. Classification of storm events (CASE)

The classification of storm events (CASE) has two steps. First, independent sample sets of storm events are defined using the observed data. Next, a threshold value, which is used to identify the storm occurrence, is derived by statistical optimisation. The common, established CASE H for the Sefton coast identifies storm events, when $Hs \geq 2.5$ m (Dissanayake et al., 2015c).

4.1.1. Selection of independent samples

Variation of the yearly storm events for the selected sample sets considering different percentile values of X (Eq. (1)) is shown in Fig. 3 in comparison to that of CASE H (blue-dash-line). The lower the percentile the higher the number of events in each year are classified as storm events. Variation of the yearly events presents an oscillatory pattern with larger number of storms around 2006/07 and 2013/14, less storms around 2009/11 and 2016/17. The number of storm events during peak years is as high as 50 for the lowest percentile (90%) sample set, while it during the trough years is as low as 5 for the highest percentile (99%) sample set. Sample sets of storm events generally show that 2013/14 was the highest year of storm occurrence, while it was 2006/07 for CASE H. Storm impacts during the 2013/14 period can be expected to result in strong erosion of the Sefton beach/dune system.

Some statistical properties of the selected sample sets of storm events are summarized in Table 3. The percentile value ($u = X\%$) varies from 2.1 to 3.6 m, which results in the average storm events per summer-summer year from 40.8 to 9.6 respectively. It should be noted that these sample sets were estimated based on the variation of X (*Eq*. 1). Therefore, the estimated events consist of high severity storm events (e.g. high *Hs* and high *TA*) as well as low severity events (e.g. low *Hs* and high *TA*), providing a large number of storm events per year. CASE H has captured about 20 storm events per year from 2005 to 2018. As mentioned in 3.1, we used a 12 h spacing between adjacent storm events to identify the meteorologically independent events. Therefore, the occurrence of the storm events of each sample set should satisfy a *Poisson* distribution. Results of the χ^2 test between the sample sets and the respective *Poisson* distributions vary from 2.9 to 6.4. These indicate that there is a variability of the independency of storm occurrence among the sample sets. The first three percentiles have lower values, implying higher independency of storm occurrence compared with the others. Moreover, the increment of the χ^2 value between two percentiles is noticeable after the third percentile (94%).

4.1.2. Optimisation of storm threshold

For the statistical optimisation of the storm threshold, the criterion of 'stability domain' is used. Variation of the shape (k) and the modified scale (σ^*) parameters indicates two stability domains (Fig. 4). The range of confidence limits (95%), which are estimated using the t-score method (Abu-Shawiesh and Saghir, 2019; Bernardara et al., 2014), increases from 0.13 to 0.22 as the number of captured storm events decreases while increasing the threshold value. The k has the first domain of stability around 0.10 from 2.35 to 2.54 m of u, and the second is around 0.07 from 2.98 to 3.07 m of the u (see domains indicated with black-dash-line in Fig. 4a). The corresponding values of the σ^* are −0.02 in the first domain and 0 in the second (Fig. 4b). The first domain indicates better stability (range ~0.19 m) than the second (range ~0.09 m), while the change of the confidence limits in the second is relatively higher than the first. It should also be noted that the bias minimization requires selection of the highest domain stability whereas the variance minimization needs more data. Our attempt is herein to select a threshold which provides a good fit between the sample storm events and the *GPD*, rather than fitting with the very extreme events only. The latter will lead to an increased fit, whereas the number of events decreases significantly neglecting the events, which are relevant for the beach/dune erosion. Accordingly, we selected the optimised threshold 2.4 m (red-dash-line: 2.395) considering the lowest increment between the points of k and σ^* within the first stability domain, which has the better stability and the lowest change in the confidence limits. A threshold value lower or higher than the optimised value results in a higher χ^2 value (see Table 3). Therefore, the selected value provides a high independency of storm occurrence. This value is then used for CASE u to identify storm events, which captures an average of 30.5 storm events per year.

Agreement of the selected storm events using $u = 2.4$ m is compared with the empirical *GPD* distribution. The selected storm events within the statistical analysis period (from 2005 to 2018) are shown in Fig. 5a with the maximum value of X (Eq. (1)) in each event and the time of occurrence. This scatter plot indicates that about 38% of the storm events have a maximum X lower than 3 m, while there are about 80% events lower than 4 m. A few very extreme events (e.g. $X > 6$) are also shown. Colour-coding illustrates the duration of each storm event in Fig. 5a. The majority of the events (72%) occur within a period smaller than one-day (24 h), and about 50% of the events have durations lower than 12 h. Only four storm events have durations more than 4 days, and their maximum X varies from 4.0 to 7.1 m. CASE u thus captures storm events with a wide range of severity levels with respect to the occurrence of high *Hs* and high *TA*, and the durations. Agreement between the

Table 2
Number of simulations (see storm events in Table 5) for FR and NR scenarios in two classifications, 1) the proposed CASE u and the established CASE H.

Scenario	CASE		Description
	u	H	
1. Fully recovered (FR)	14	9	Same initial profile
2. Not recovered (NR)	14	9	Storm impacted profile from the previous event

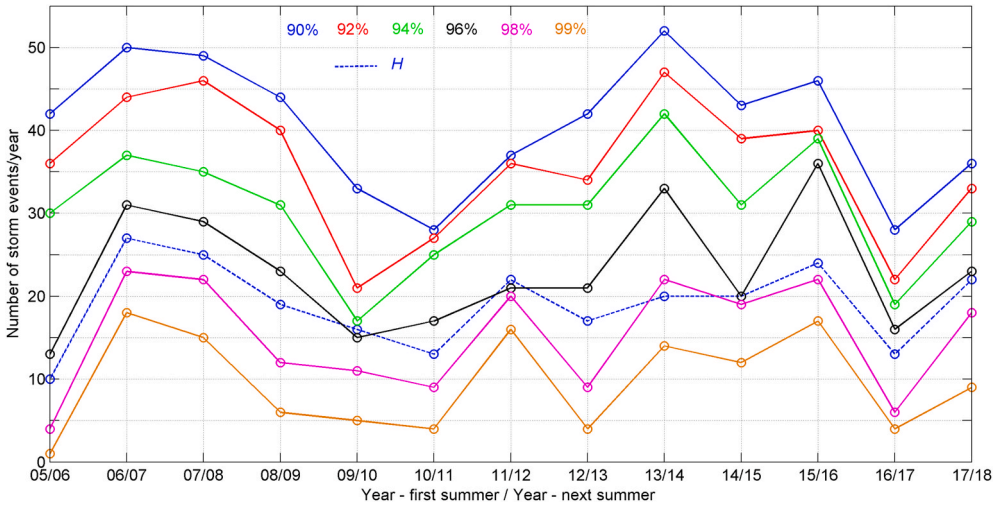

Fig. 3. Summer-Summer yearly storm events (e.g. from Sep-2005 to Sep-2006) variation from 2005 to 2018 for the selected independent sample sets (colour-coding) and for the established storm definition (H: blue-dash-line) of the Sefton coast. (For interpretation of the references to colour in this figure legend, the reader is referred to the Web version of this article.)

Table 3
Selected percentiles to develop independent sample sets of storm events for the statistical analysis, the threshold (u), the averaged storm events per year and the $\chi 2$ test value by comparing the sample sets with the Poisson distribution.

%	$u = X$% (m)	Averaged events/year	$\chi 2$ value
90	2.1	40.8	2.9
92	2.2	35.8	3.8
94	2.4	30.5	3.5
96	2.7	22.9	4.9
98	3.2	15.2	7.8
99	3.6	9.6	6.4

selected storm events and the theoretical *GPD* ($\sigma = 0.2291$, $k = 0.1064$ for *Eq.* 4) is analysed using a probability plot (Fig. 5b). The sample points of storm events (black-circle) follow the theoretical *GPD* curve (red-line) more than 4 m of *X*, indicating a better agreement between the samples and the distribution. Thereafter, the samples deviate from the *GPD* curve, whereas they tend to progress close to the distribution up to about 6 m of *X*. The very extreme storm events which were found in the scatter plot, show relatively large deviations with the *GDP* curve.

The overall agreement between the sample storm events and the *GPD* distribution is analysed with the statistical parameters (Table 4). The values of the statistical parameters indicate that there is a good agreement between the selected storm events and the respective *GPD*.

If both CASE *u* and *H* are used to identify storm occurrence in the period 2005–2018, CASE *u* identifies 397 events, while it is 248 events for CASE *H*. Obviously CASE *u* defines additional 49 events (37%) as storms. In the simulation period (September 10–December 09, 2013), the characteristics of the identified storm events are summarized in Table 5. There are 14 storm events with longer durations in CASE *u* compared to 9 events in CASE *H*. Therefore, CASE *u* has identified 5 additional events (S2, S3, S5, S6 and S10), which is about 35% than CASE *H*. The highest water level of the additional events is found in S6, while the highest wave height is shown in S10. S6 spanned 11 h, the

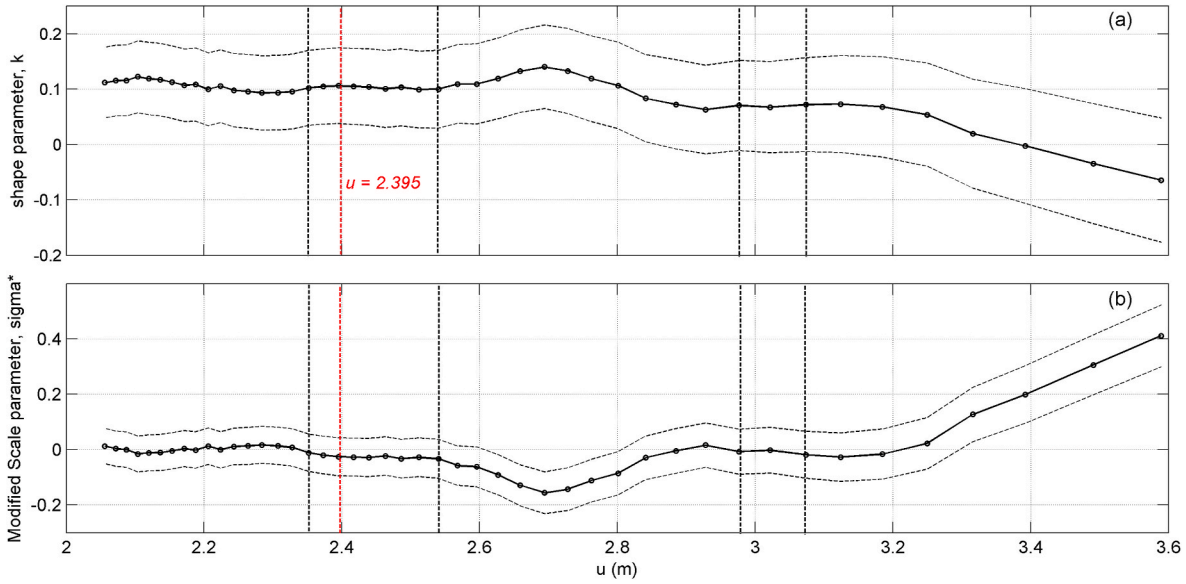

Fig. 4. Variation of the Shape, *k* (a) and the Modified Scale, σ^*(b) parameters of the Generalized Pareto Distribution with the 95% confidence limits. Stability domains are indicated by black-dash-line and the selected optimised threshold is shown by the red-dash-line. (For interpretation of the references to colour in this figure legend, the reader is referred to the Web version of this article.)

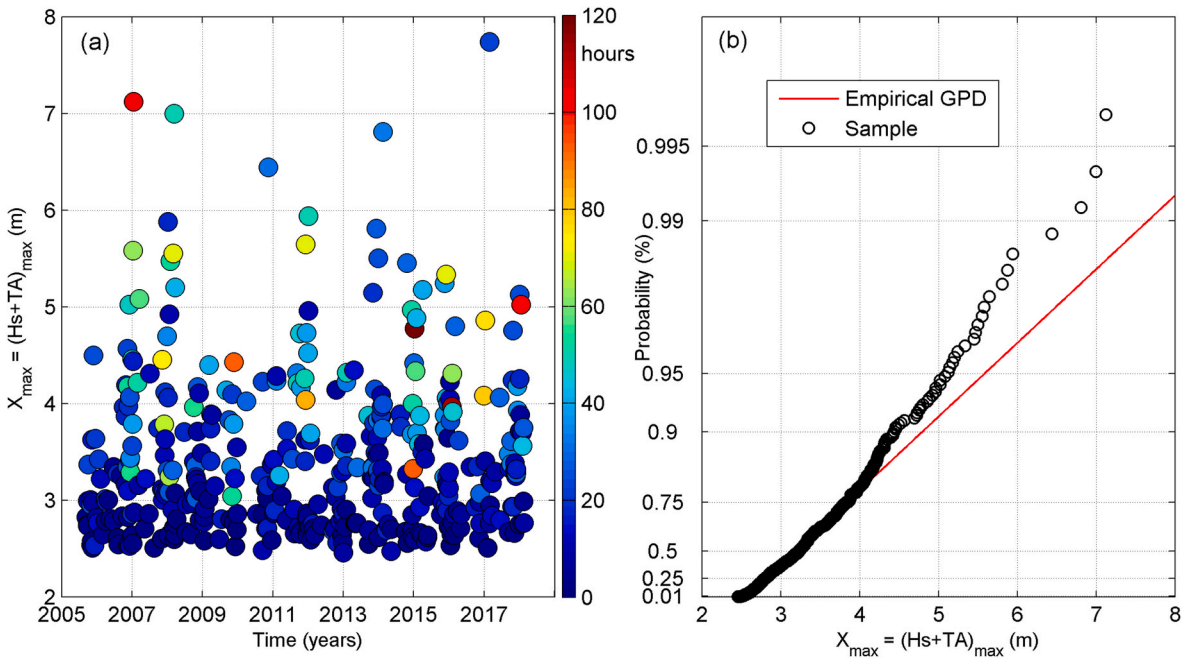

Fig. 5. Selected storm events using CASE $u = 2.4$ m with the maximum of X during each event vs time in years (a) and the colour-coding indicates storm durations in hours. Agreement of the empirical *GPD* and the sample storm events is shown with the *GPD* probability vs maximum X (b). Black-circles are the sample storm events and the red-line is the empirical *GPD*. (For interpretation of the references to colour in this figure legend, the reader is referred to the Web version of this article.)

Table 4
Statistical comparison between the sample storm events from 2005 to 2018 and the empirical GPD.

Parameter		CASE $u = 2.4$ m
Variance (m^2)	Sample	0.08
	GPD	0.05
Bias (m)		0.02
RMSE (m)		0.07
R^2 (−)		0.96

peak wave height of 2.4 m occurred at high water tide of 4 m, and the peak water level was at 4.3 m with a *Hs* of 2.2 m S10 spanned 7.5 h, the peak wave (2.7 m) occurred at low water tide (−2 m), whereas the peak water level was at high water tide (4.2 m) with a *Hs* of 2.3 m. Therefore, these 5 events could provide non-negligible impacts of erosion along the profile (Fig. 1d), which are relevant to estimate the storm erosion.

From the identified storm events within the statistical analysis and the simulation periods, it is evident that CASE *u* is able to capture about 35% of additional events than CASE *H*. Therefore, the storm events of CASE *u* could provide potentially high storm impacts leading to a comprehensive investigation of storm erosion.

4.2. Storm erosion

Storm erosion is estimated by forcing the 1D model domain (see Fig. 1c) using the derived storm events in both CASEs following the two hypothesized scenarios, 1) FR and 2) NR (Table 2). Of the additional events in CASE *u*, S6 has the highest water level (4.3 m). Therefore, we first select this event as an example to investigate the event-based storm erosion. Then, the dune toe level change and the storm erosion volume of each individual event are compared between CASE *u* and *H*. Finally, the overall simulated storm erosion during the simulation period is compared to the measured profile data.

4.2.1. Event-based storm impact

The profile evolution during S6 is shown in Fig. 6 with the initial and final measured profiles. For clarity, only the segment covered by the measured profiles is herein considered. In FR (Fig. 6a), the final simulated profile (green-line) indicates the storm impacted erosion at the ridges and at the dune front. The maximum erosion at the ridges is about 0.2 m (at about 370 m landward distance), which is nearly 50% of the erosion compared with the final measured profile (red-line), and the runnel areas have experienced accretion (Fig. 6c). The bed level change within the upper beach is higher than the lower beach. The maximum erosion at the dunes is about 0.3 m during S6 (at 515 m landward distance in Fig. 6d). However, during the entire period from September 10 to December 09, 2013, this area has experienced accretion and lowering the upper dune face (see measured profiles: red-line and black-dash-line in Fig. 6d). In NR (Fig. 6b), the simulated final profile of the previous event (S5) was used as the initial profile. There is no prominent ridge-runnel pattern on the initial profile as in FR. The initial profile quite agrees with the final measured profile within the upper beach, and thus a marginal erosion occurred in this area. Furthermore, the initial profile indicates that the dune front has partly eroded during the impacts of the previous storm events (i.e. see black-dash-line in Fig. 6d and e). Therefore, the erosion at the dune front is also lower (<0.2 m) than that in FR.

The simulated profile at Formby Point is surrounded by dunes of higher elevations (maximum height ~ 20 m), and the ridge-runnel pattern extends nearly parallel to the shoreline along the coast. The erosion of the lower dune triggers lowering of the upper dune face due to the steep gradient of the profile (see Fig. 6d and e). Thus, the simulated vertical erosion values (0.2 at the ridge-runnel and 0.3 at the dune) could result in high erosion volume within the Formby Point area. Obviously, the S6 event has considerable impact on the beach/dune erosion, and needs to be considered while evaluating the storm erosion.

The elevation at dune toe changes depending on storm erosion. If erosion occurs at dune toe, the elevation decreases. However, erosion at the dune face could result in increase or even no change at the dune toe level due to slumping and avalanching processes. The change of dune toe elevation is compared between the simulated profiles in FR and the 5 dune toe surveys around Formby Point (Fig. 7). On the initial profile of the model (September 10, 2013), the dune toe level is at 4.25 m, while it

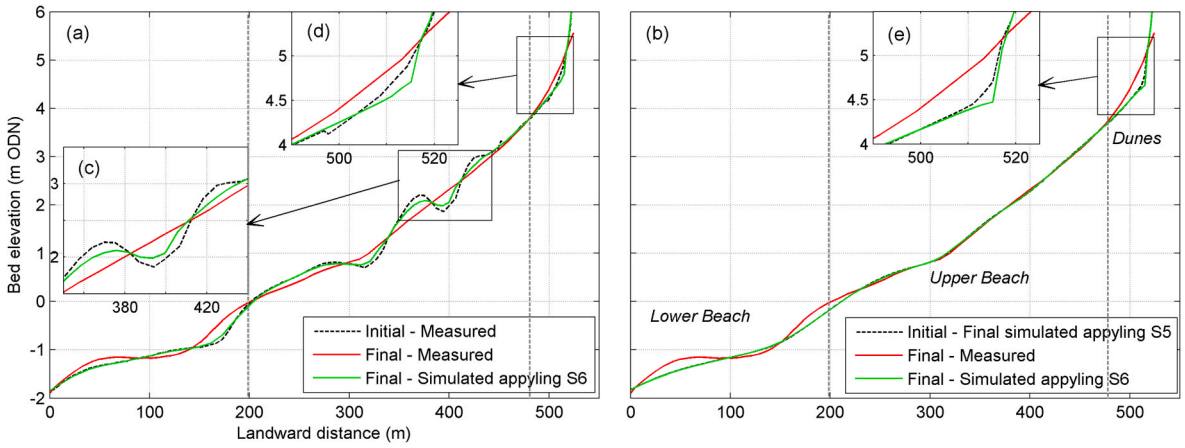

Fig. 6. Comparison of profile evolution during S6 (additional event of CASE *u*), in FR (a) and NR (b) (Table 2). Beach/dune profile is shown only for the segment of the measured profiles. The final measured profile is included as a reference to compare erosion during S6.

is about 4.7 m south and 4.6 m north of Formby Point with the dune toe survey on September 18, 2013. It should be noted that the S1 event on September15–September 17, 2013 could increase the elevation at dune toe by eroding material coming from the upper dunes. Furthermore, the measured dune toes have about 10 m alongshore resolution. Therefore, the dune toe survey may have not captured the exact location of the profile measurement. Colour-coding of the surveyed dune toes indicates that the elevation increases from autumn (blue-line) to winter (black-line). Similar observation is found with the model predicted change at the dune toe, which implies increased storm erosion at the dune face from autumn to winter. Of the 9 events present in both CASEs (see Tables 5) events show increase at the dune toe level (note. $S4_u$ has higher increase than $S4_H$). S6 and S10 of the additional events captured in CASE *u* have also increased the dune toe elevation. These results indicate, only some events are susceptible to the dune toe change, and the vulnerable events in CASE *u* is higher than in CASE *H*.

The simulated erosion volume of each storm event in FR and NR is then compared between CASE *u* and *H*. In FR, the impact of each storm event was simulated using the measured initial profile. The erosion volumes in the lower beach (Fig. 8a) are considerably lower than the upper beach (Fig. 8b). This is a twofold effect. The extension of the lower beach is shorter than the upper beach, and the upper beach consists of a prominent ridge-runnel pattern, which provides strong interactions between the approaching storm wave and the bed topography. The storm events of CASE *u* generally show higher erosion volumes in both lower and upper beaches compared with CASE *H*. Only two events in CASE *H* (i.e. S4 and S9) cause increased erosion (within the upper beach) compared to CASE *u*. Durations of S4 and S9 in CASE *u* are longer by 0.5 and 4.5 h respectively than those of *H* (Table 5). It can be expected that the longer durations of these two events in CASE *u* caused increased transport of the eroded sand from the dune up to the upper beach, resulting in the reduced erosion of the upper beach. This is evident by higher erosion at the dune and in the lower beach in CASE *u* than in CASE *H* (Fig. 8a and c). S6 causes particularly strong erosion along the entire profile, which is even higher than some events captured by both CASEs (e.g. S4, S7). It is therefore shown that CASE *u* has captured

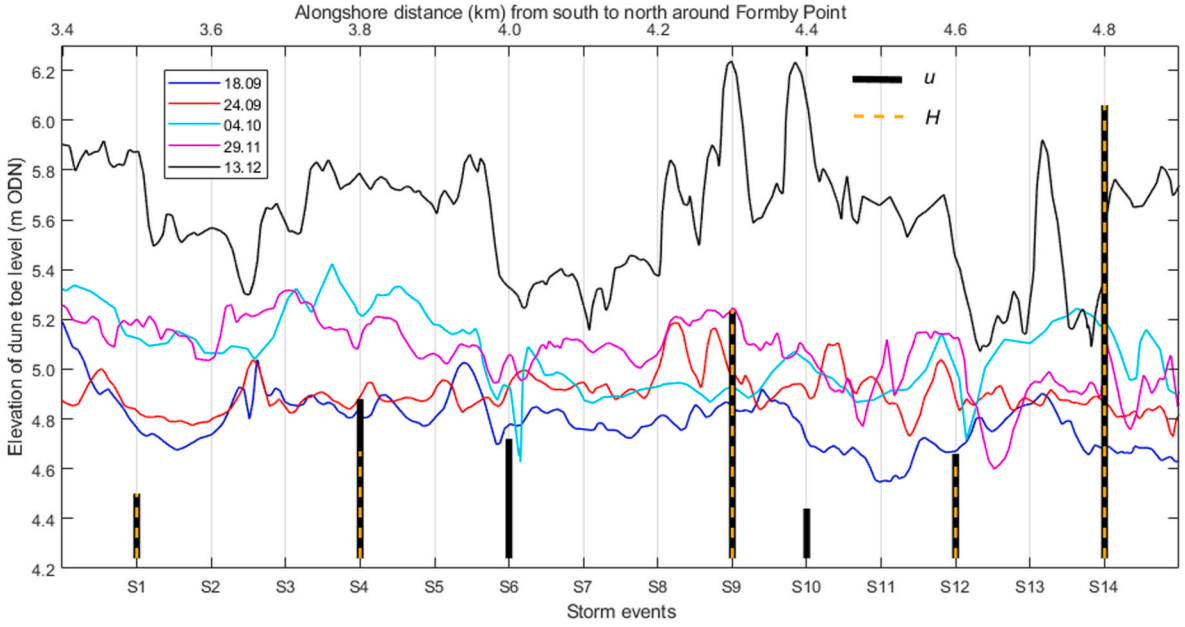

Fig. 7. Model simulated dune toe level change (note. initial dune toe is at 4.25 m: FR) during storm events (CASE *u*: thick-black-line and CASE *H*: yellow-dash-line) with the measured dune toe levels (colour-coding) around Formby Point enclosing the simulation period (September 10–December 09, 2013). Alongshore distance indicates from south to north based on the dune toe surveys. (For interpretation of the references to colour in this figure legend, the reader is referred to the Web version of this article.)

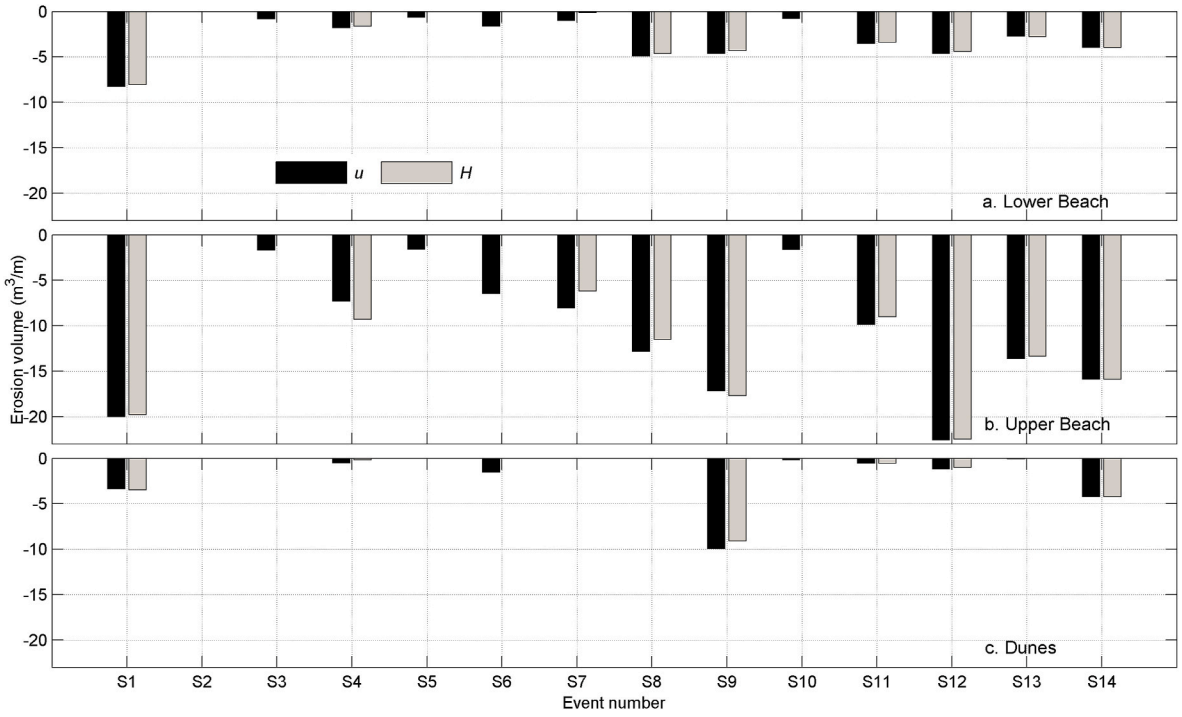

Fig. 8. Model simulated erosion volume within the measured profile segment (see Fig. 6) considering that the profile is fully recovered (FR) between storm events; Lower Beach (a), Upper Beach (b) and Dunes (c). Additional events captured in CASE *u* are S2, S3, S5, S6 and S10.

Table 5
Characteristics of the selected storm events during the simulation period from September 10 to December 09, 2013 using CASE u and H. CASE u has captured 5 additional events (S2, S3, S5, S6, S10).

Storm ID	CASE *u*						CASE *H*					
	Period		Duration	Spacing	Hs, peak (WL)	WL, peak (Hs)	Period		Duration	Spacing	Hs, peak (WL)	WL, peak (Hs)
	Start	End	(hr)	(days)	m (m)	m (m)	Start	End	(hr)	(days)	m (m)	m (m)
S1	2013-09-15 10:00	2013-09-17 07:00	45		3.4 (−1.9)	4.2 (2.8)	2013-09-15 13:30	2013-09-17 07:00	41.5		3.4 (−1.9)	4.2 (2.8)
S2	2013-09-18 16:00	2013-09-18 17:30	1.5	1.4	2.3 (−3.4)	−3.1 (2.3)						
S3	2013-09-19 12:30	2013-09-19 19:30	7	0.8	2.2 (−2.8)	3.2 (2.1)						
S4	2013-10-09 13:30	2013-10-10 00:00	10.5	19.8	3.3 (−1.1)	4.6 (2.2)	2013-10-09 14:00	2013-10-10 00:00	10	22.3	3.3 (−1.1)	4.5 (2.5)
S5	2013-10-16 15:30	2013-10-16 18:30	3	6.6	2.5 (0.8)	1.7 (2.4)						
S6	2013-10-23 09:00	2013-10-23 20:00	11	6.6	2.4 (4.0)	4.3 (2.2)						
S7	2013-10-27 08:00	2013-10-27 20:00	12	3.5	2.5 (2.1)	2.9 (2.3)	2013-10-27 12:30	2013-10-27 18:30	6	17.5	2.5 (2.1)	2.1 (2.5)
S8	2013-10-28 09:00	2013-10-29 18:00	33	0.5	2.9 (−0.9)	2.6 (2.2)	2013-10-28 11:30	2013-10-29 15:30	28	0.7	2.9 (−0.9)	−0.8 (2.5)
S9	2013-11-02 15:00	2013-11-03 11:30	20.5	3.9	4.4 (2.5)	5.2 (3.8)	2013-11-02 18:00	2013-11-03 10:00	16	4.1	4.4 (2.5)	5.2 (3.8)
S10	2013-11-05 15:30	2013-11-05 23:00	7.5	2.2	2.7 (−2.0)	4.2 (2.3)						
S11	2013-11-13 21:30	2013-11-14 17:00	19.5	7.9	3.5 (0.6)	3.4 (3.0)	2013-11-14 00:30	2013-11-14 18:30	18	10.6	3.5 (0.6)	3.4 (3.0)
S12	2013-11-20 03:00	2013-11-21 04:30	25.5	5.4	3.8 (1.6)	4.3 (3.3)	2013-11-20 03:30	2013-11-21 05:00	25.5	5.4	3.8 (1.6)	4.3 (3.3)
S13	2013-11-29 07:30	2013-11-30 01:00	17.5	8.1	3.2 (−1.9)	3.2 (2.9)	2013-11-29 08:00	2013-11-30 02:00	18	8.1	3.2 (−1.9)	3.2 (2.9)
S14	2013-12-05 03:30	2013-12-06 07:00	27.5	5.1	4.6 (6.2)	6.2 (4.6)	2013-12-05 03:30	2013-12-06 07:00	27.5	5.1	4.6 (6.2)	6.2 (4.6)

additional storm events, which enable considerable erosion of the beach/dune system at Formby Point.

For NR, the simulated erosion volumes are shown in Fig. 9. The highest erosion in the lower and upper beaches, and also erosion at the dune occurred during the first storm event (S1), which lasted for 45 and 41.5 h in CASE *u* and *H* respectively. CASE *u* results in higher erosion due

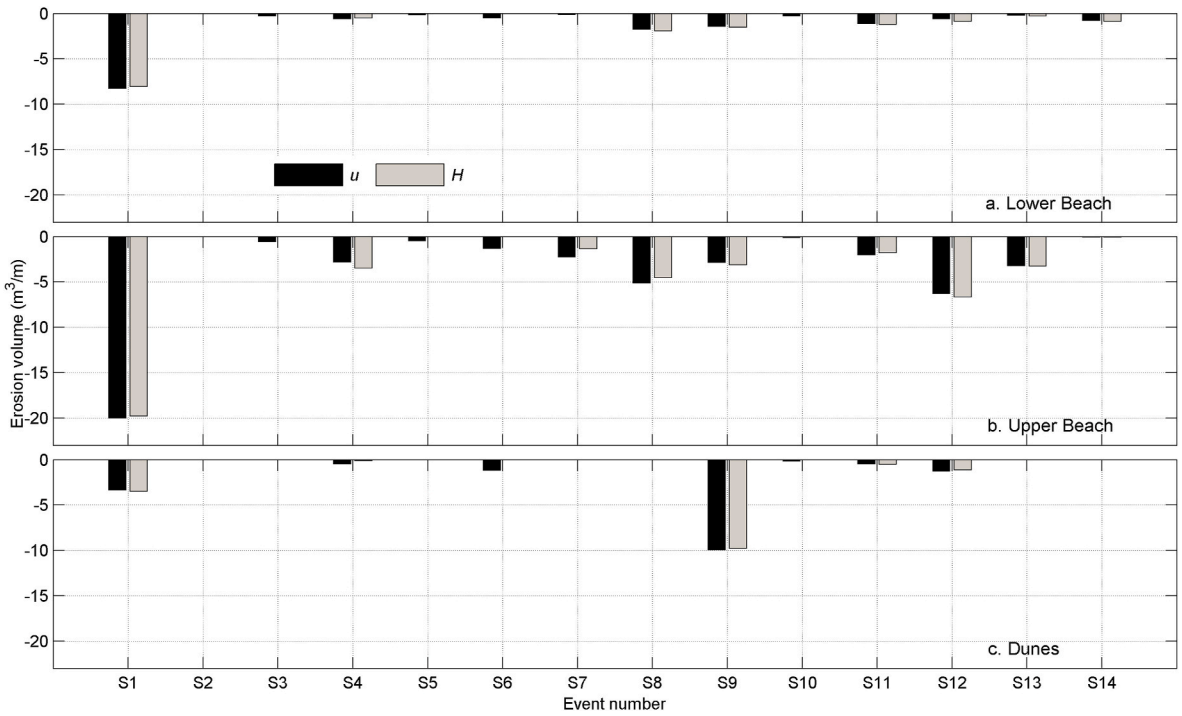

Fig. 9. Model simulated erosion volume within the measured profile segment (see Fig. 6) considering that the profile is not recovered (NR) between storm events; Lower Beach (a), Upper Beach (b) and Dunes (c). Additional events captured in CASE *u* are S2, S3, S5, S6 and S10.

to longer duration of S1 than *H*. In the other events besides S9, the erosion volumes within the three regions of the profile are remarkably lower than that of S1. In S9, water level reached up to 5.2 m coinciding with a *Hs* of 3.8 m (see Table 5). The highest water level of the first eight events (from S1 to S8) was only 4.6 m, and the corresponding *Hs* was only 2.8 m. Therefore, S9 has particularly strong impact on the dune resulting to the highest erosion. During the impacts of S1, the ridge-runnel pattern has been significantly flattened and thus low erosion volumes are shown in the lower and upper beaches for the subsequent events. The additional storm events in CASE *u* also show erosion in the lower and upper beaches, and on the dune (e.g. S6). It should be noted, after S6, the events of CASE *u* could produce lower erosion than *H*, because the profile is already impacted by the additional events. The results of CASE *u,* however, indicate that the erosion volumes of the events after S6 have comparable or higher erosion than *H*. S14 shows no erosion of the dune though water level reached up to 6.2 m with a *Hs* of

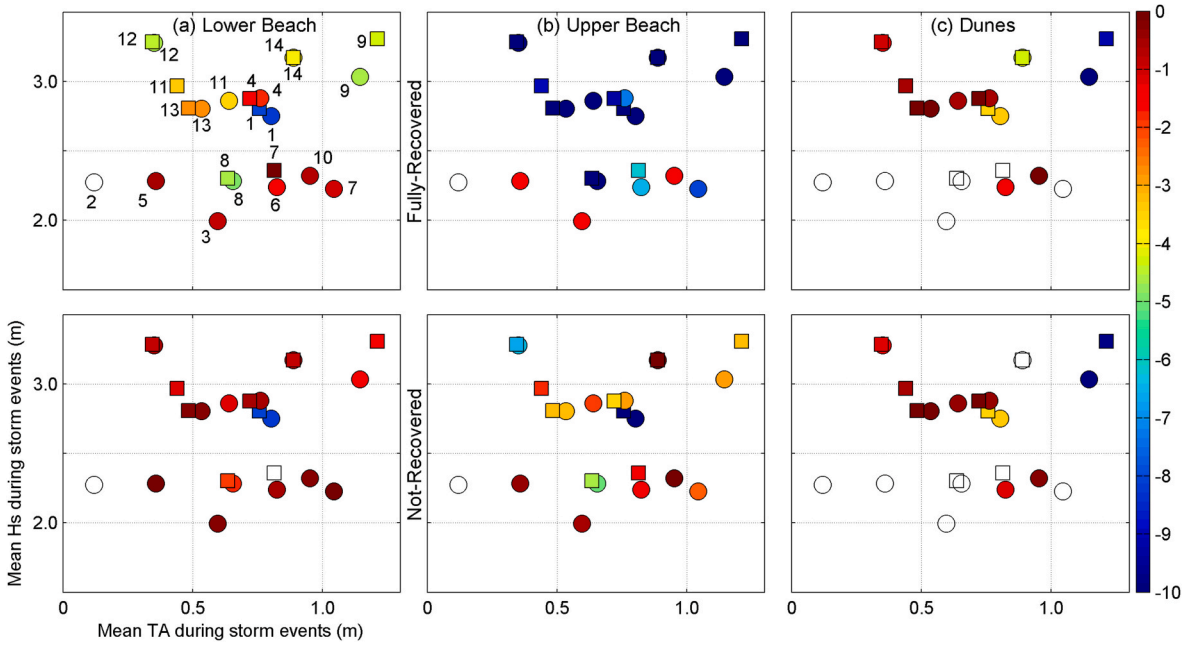

Fig. 10. Erosion volume with the mean *Hs* vs the mean *TA* during storm events in the Fully-Recovered (FR: Upper panels) and the Not-Recovered (NR: Lower panels) simulations. Numbers on the upper-left plot are referred to the storm events (see Table 5), from CASE *u* (○) and CASE *H* (□), and colour-coding indicates erosion volume (m^3/m) and white-colour indicates no erosion. Vertical panels are Lower Beach (a), Upper Beach (b) and Dunes (c). (For interpretation of the references to colour in this figure legend, the reader is referred to the Web version of this article.)

4.6 m. This suggests that the dune is already eroded and set back during the previous events, particularly with the impact of S1 and S9. Similar to FR, the results of NR also indicate that capturing additional events in CASE *u* (e.g. S6) impacts the beach/dune erosion at Formby Point.

Sensitivity of the simulated erosion volumes to the variations of water levels and wave heights is analysed using the mean values of *TA* ($\overline{TA}$) and *Hs* ($\overline{Hs}$) during the storm events as proxies (Fig. 10).

$\overline{Hs}$ varies from 2 to 3.3 m, while $\overline{TA}$ ranges from 0.1 to 1.2 m. The additional storm events of CASE *u* (S2, S3, S5, S6 and S10) have lower $\overline{Hs}$ than 2.5 m. Both maximum $\overline{TA}$ (1 m) and $\overline{Hs}$ (2.3 m) of the additional events are found with S10. However, S6 shows the maximum erosion in FR and NR (see change in colour-coding in S6 and S10). Longer storm duration of S6 (11 h) than S10 (7.5 h) has resulted in higher erosion but lower $\overline{Hs}$ and $\overline{TA}$. S7, S9 and S11 have relatively large differences of $\overline{TA}$ and $\overline{Hs}$ between two CASEs. These events have longer storm durations in CASE *u* than *H* (see Table 5). In $S7_u$, $\overline{TA}$ is higher by 0.2 m, but $\overline{Hs}$ is lower by 0.1 m than $S7_H$. $S7_u$ has higher erosion within the lower and upper beaches compared with $S7_H$. $S11_u$ has also higher $\overline{TA}$ (0.2 m), but lower $\overline{Hs}$ (0.1 m) than $S11_H$. The erosion volumes of $S11_u$ are higher than $S11_H$. In $S9_H$, $\overline{Hs}$ and $\overline{TA}$ are higher by 0.3 m and 0.1 m respectively than $S9_u$. However, $S9_u$ shows higher erosion than $S9_H$. This occurs due to the longer storm duration of $S9_u$ (20.5 h) compared with $S9_H$ (16 h). Therefore, these results indicate that *TA* dominates on the beach/dune erosion compared to *Hs*, while the longer the storm duration, the higher the erosion though $\overline{Hs}$ and $\overline{TA}$ decrease.

4.2.2. Overall storm impact

The overall evolution of the profile is compared between the measured and simulated profiles using the initial and final profiles of the simulation period (September 10–December 09, 2013). The initial and final measured profiles are shown in Fig. 11 with the final simulated profiles. The measured profiles (black-dash-line: initial and red-line: final) indicate strong erosion at ridges and sedimentation at runnels due to the storm impacts. This is particularly found in the profile segment from 0.8 to 3.0 m of the upper beach, where the ridge-runnel pattern is prominent. In FR (Fig. 11a), the initial and final profiles of S14 (last event) are analysed (note. both S1 and S14 have the same initial profile). In NR (Fig. 11b), the initial profile of S1 and the final profile of S14 are analysed. In both scenarios, the final simulated profiles of CASE *u* (green-line) and *H* (blue-dash-line) have qualitatively the same variation as the measured final profile (*RMSE*~0.15 m and *BSS*~0.3). The segment from 0.8 to 3.0 m ODN agrees much better between the measured and the simulated profiles of the two CASEs and also the scenarios (*RMSE*~0.09 m and *BSS*~0.8). Simulated profiles in FR and NR indicate accretion at the dune (~4–5 m elevation). It should be noted that the measured profile extends up to about 5.5 m elevation, and so does the comparison. Above this level (>5.5 m), both final profiles (measured and model) indicate erosion compared with the initial profile. The maximum dune height along this profile reaches about 20 m. Therefore, during the storm impacts, the upper dune has been eroded (slumping of the dune front) resulting accretion at the lower dune. This is a common phenomenon of dune erosion (slumping and avalanching). The simulations have over-predicted dune erosion, though the trend agrees with the measured data. In FR (Fig. 11a), both CASEs have similarly captured S14 (see Table 5). Therefore, both the green-line (*u*) and the blue-dash-line (*H*) show exactly the same pattern. In NR (Fig. 11b), the profiles have experienced cumulative impacts of erosion. In CASE *u*, the final profile is resulted from the impacts of 14 events, while it is only 9 events in CASE *H*. At the upper beach (Fig. 11c), the green-line (*u*) is below the blue-dash-line (*H*). At the dune (Fig. 11d), the green-line is smooth compared with the blue-dash-line. These indicate the higher impact of CASE *u* than *H*, though they are marginal. It is also shown that the erosion along the profile is lower in FR than NR. For example, at the distance 250 m, the simulated profiles are above the measured final profile (red-line) in Fig. 11a (FR), while they are below in Fig. 11b (NR). Moreover, on the dune, the difference between the measured and the simulated profiles is higher in FR than NR (e.g. see at 5 m). These results indicate, neither the number of storm events within the simulation period nor the durations of the events in CASE *u* and *H* are able to produce significant different of the final profile, whereas the two hypothesized scenarios show different impacts due to the cumulative effects.

The overall erosion volume within the simulation period is estimated considering the initial and final profiles of the measured data and the simulated results (Fig. 11). The estimated overall erosion volumes are shown in Fig. 12 for the lower and upper beaches, and the dune separately. Within the lower beach, the estimation from the measured profiles has an erosion volume of 3.4 m^3/m, while it is 4.0 m^3/m for FR in both CASEs. In NR, the lower beach has experienced erosion volumes of 13.3 and 12.4 m^3/m for CASE *u* and *H* respectively. These results indicate that the simulated erosion volumes of FR (during S14) resemble the estimated erosion from the observations. The erosion of the upper beach is greater than the lower beach (note. the profiles of the lower beach encounter only a part of the lower beach from 0 to −1.8 m). The measured profiles within the upper beach result in erosion of 26 m^3/m, while it is 16 m^3/m in FR for both CASEs, and that of NR is 37.7 m^3/m for CASE *u* and 36.1 m^3/m for *H*. Therefore, the simulated erosion in FR is under-predicted and in NR is over-predicted by about 10 m^3/m in both CASEs compared with the erosion from the observations. The lowest erosion of the measured profiles is found on the dune (2.9 m^3/m). The dune erosion of FR is 4.2 m^3/m in both CASEs, while it is fairly same in

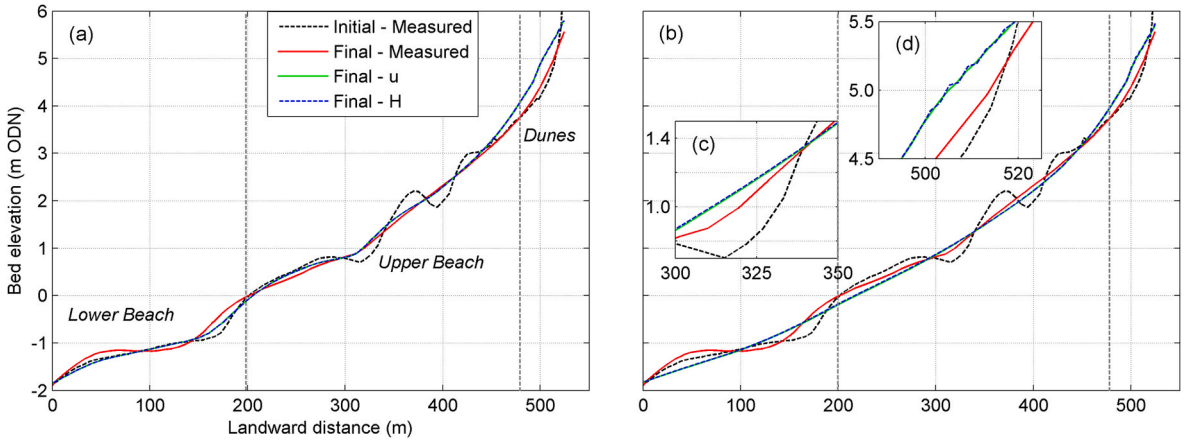

Fig. 11. Comparison of the measured and simulated final profiles within the simulation period (September 10–December 09, 2013), by forcing with the storm events of CASE *u* and *H* in the fully recovered, FR (a) and the not recovered, NR (b) scenarios.

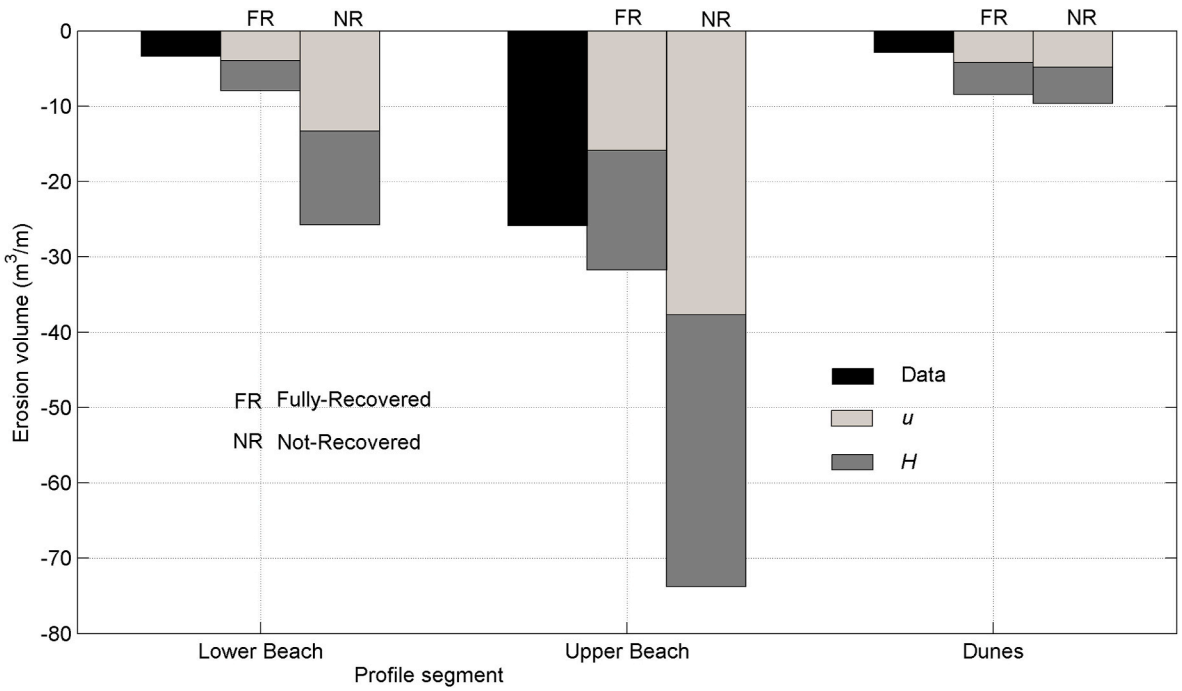

Fig. 12. Overall erosion volume during the simulation period of storm events (September 10–December 09, 2013) within the measured profile segment (see Fig. 11) in the simulations of Fully-Recovered (FR) and Not-Recovered (NR) scenarios. Black-colour-bar: observations, light-colour-bar: CASE *u*, and dark-colour-bar: CASE *H*. CASEs *u* and *H* are stacked on each other, *H* does not start from the *x*-axis.

CASE *u* (4.9 m^3/m) and *H* (4.8 m^3/m) of NR.

The overall evolution of the profile during the simulation period suggests that the hypothesized two scenarios provide the lower (FR) and the upper (NR) bounds of the storm driven beach/dune erosion. The final profile, particularly from 0.8 to 3 m ODN, does not depend on the number of storm events or the storm durations, but it is related to the severity of the storm events. Therefore, in the overall storm impact considering the initial and final profiles of the simulation period, both CASE *u* and *H* result in fairly similar storm erosion. If the overall erosion volume is estimated based on the event-based erosion (4.2.1), the simulated erosion volume of CASE *u* is higher by 12% (FR) compared with CASE *H*. Therefore, the difference in storm impact between CASE *u* and *H* is noticeable in FR while analysing the event-based erosion.

5. Discussion

The established CASE for the Sefton coast (*H*) is based on wave heights only (i.e. $Hs \geq 2.5$ m), although it is a hyper-tidal environment (spring tidal range ~ 10 m). This CASE has been used in several studies as the basis to identify the occurrence of storm events and to investigate the storm impacted beach/dune erosion (Williams et al., 2011; Dissanayake et al., 2015a,b,c; Karunarathna et al., 2018). Storm driven erosion of the Sefton beach/dune system increases when storm waves approach the coast during high water (Pye and Blott, 2016). The occurrence of storm events at spring low water provides minimal impacts on the beach while resulting in episodic erosion of the dune, if storm events coincide with the highest water level during spring. Therefore, the CASE using wave heights alone does not necessarily identify all extreme events, which are of relevance for the storm driven beach/dune erosion. This raises the requirement of investigating the beach/dune erosion resulting from the events of a classification, which uses both wave heights and water levels (CASE *u*).

We used the offshore wave heights (*Hs*) and the nearshore water levels (*TA* = observed tide-astronomical tide) to propose a novel CASE for the Sefton coast and to investigate the storm erosion at beach/dune. Our basis is the occurrence of high *Hs* and high *TA*, which can be expected during storm events (Haigh et al., 2016; Pye and Blott, 2016). Quartel et al. (2007) employed *Hs* and *TA* with two separate thresholds to identify the storm events, which disturb the gradual bar migration, using the Argus video images at Noordwijk, the Netherlands. Dune erosion was beyond the focus of this analysis, and many beach/dune systems are not rich with the Argus images. Li et al. (2014) used this bivariate threshold method to define storm events. They adopted an arbitrary threshold for *Hs* and the proposed *TA* by Quartel et al. (2007) for their probabilistic analysis of storm occurrence. In contrast, we developed a single threshold for both parameters using a combined approach of the univariate function (Bernardara et al., 2014) and the bivariate analysis (Mazas and Hamm, 2017). In the bivariate analysis of Mazas and Hamm (2017), the univariate function was defined using the nearshore water levels and the nearshore wave heights, which were obtained by transforming the offshore wave heights into the nearshore area using analytical formulas (Goda, 2010). These formulas describe wave transformation by refraction and shoaling processes considering a uniform bathymetry with shore parallel depth contours. The Sefton coast has a convex-shape and a complex bathymetry. Furthermore, Coco et al. (2014) showed that the offshore wave characteristics are responsible for the beach/dune erosion. Therefore, our analysis used offshore *Hs*, and this was subsequently used to force the XBeach model, which has advanced wave transformation processes (Roelvink et al., 2009).

Occurrence of storm events, which are relevant for the beach/dune erosion, was identified using statistical analyses. The time spacing between adjacent events was set to more than 12 h. It is higher than the period of the transitory *TA*s generated by storm tracks over the Irish Sea (Brown et al., 2010a). For the southern North Sea, the storm spacing of 6 h has been used (Li et al., 2014). Storm tracks pass generally over the British isle and approach the North Sea (see Fig. 4 in Haigh et al., 2016). Therefore, the selected storm spacing should satisfy for the meteorologically independent events on the Sefton coast. This was further confirmed with the low χ^2 values between the sample events and the *Poisson* distribution (Table 3). Variation of the yearly storm events had an oscillatory pattern (Fig. 3). The crests and the troughs indicated high and low storm occurrence respectively. They correspond to positive

(NAO^+) and negative (NAO^-) North Atlantic Oscillations, which depend upon the location of storm tracks over the north Atlantic ocean (Schlichtholz, 2018). For the statistical optimisation of the storm threshold, we used the two-parameter *Generalized Pareto Distribution* (*GPD*) following the Pickland's theorem (Pickland, 1975). The *GPD* has improved properties for the extreme value analysis compared with the other extreme value families, *Gumbel*, *Fréchet* and *Weibull* (Li et al., 2014; Callaghan et al., 2008). The optimised threshold ($u = 2.4$ m) captured about 30 events annually, which had a good agreement with the *GPD* (*RMSE* = 0.07 m in Table 4). Using bivariate thresholds, Li et al. (2014) identified more than 30 events annually for the North Sea, and Mazas and Hamm (2017) suggested to use 15–25 average events per year for time series (*Hs*, *TA*) of about 10 years. Therefore, the optimised threshold has captured reasonable number of storm events. The agreement between storm events and *GPD* slightly increased for high threshold values whereas the captured events significantly decreased (e.g. $u = 3.6$ m, 10 events/year, *RMSE* = 0.03 m). Such events are however very extreme events with high return levels (e.g. 2013/14 winter: Haigh et al., 2016), and are important for estimating coastal flooding (McMillian et al., 2011) or the impacts at coastal structures (Bruce et al., 2009). Our focus in this study was to investigate the storm driven beach/dune erosion. Selecting a high threshold thus results in neglecting the events, which are severe enough to impact the beach or cause dune erosion. Dissanayake et al. (2019a) showed that the storm events with low wave height and high water level are as important as the events with high wave heights and low water level for the beach/dune erosion. The derivation of CASE *u* enabled selection of those very extreme events together with lower severity events.

The proposed CASE *u* identified additional storm events (35%) compared with the established CASE *H* in both statistical analysis and simulation periods. Therefore, the occurrence of events per year is higher in CASE *u* than *H*. Haigh et el. (2016) described that the 2013/2014 winter had the largest number of extreme events within the last 100 years. CASE *u* was able to capture this observation (94% in Fig. 3). However, CASE *H* showed that 2006/07 had the largest number of events. During the increasing phase of storm occurrence (e.g. from 2009/10 to 2013/14 in Fig. 3), the increase of storm events per year is higher in CASE *u* than *H*, and that indicates the global changes are better captured by CASE *u*. Moreover, Dissanayake et al. (2019a) showed, when a storm event with *Hs* of 2 m occurs during high water tide (e.g. MSL+2 m) at Formby Point, results in higher erosion than an event with *Hs* of 2.5 m at MSL. CASE *u* is able to capture both of these events whereas CASE *H* can identify only the latter event. Furthermore, the occurrence of a high severe event after a low severe event causes higher erosion at Formby Point than the occurrence of the high severe event alone (Dissanayake et al., 2015c). This indicates the importance of capturing low severe events (e.g. $Hs < 2.5$ m) because they modify the ridge-runnel pattern in the inter-tidal area allowing to direct impact of a subsequent high severe event at dunes. Splinter et al. (2014) also showed that storm erosion of several low sever events is important over a high severe event.

Two hypothesized scenarios representing inter-storm beach recovery were adopted for the numerical simulations (XBeach) at Formby Point, which shows the highest vulnerability to storm impacts on the Sefton coast (Esteves et al., 2011; Dissanayake et al., 2014; Pye and Blott, 2016). The simulation period was based on the two surveyed profiles on 10.09 and December 09, 2013, and we identified therein several storm events (CASE *u*: 14 and *H*: 9). Therefore, the two profiles do not represent pre- and post-storm status of the individual events, whereas the evolution of the entire simulation period. XBeach is a dune erosion model, which has proven capacity in predicting storm driven beach/-dune erosion (Roelvink et al., 2018). During calm periods between storm events, beach/dune recovery processes are likely to occur either partially or fully (Pender and Karunarathna, 2013). Since XBeach cannot predict recovery processes for the same parameter setting as of the storm erosion (Bart, 2017) and the availability of only two profiles, we hypothesized two scenarios to bound the uncertainty due to system recovery: 1) the profile is fully recovered (FR) and 2) the profile is not recovered (NR) during the inter-storm calm periods, to simulate the storm driven beach/dune erosion.

The event-based storm impact resulted in higher erosion in CASE *u* in both scenarios than CASE *H*. In FR, each storm event impacted on the prominent ridge-runnel pattern causing strong erosion within the lower and upper beaches. It was found that the many events of CASE *u* resulted in higher erosion volumes compared with CASE *H* (Fig. 8). Longer storm durations of the events in CASE *u* (see Table 5) provided increased impact and in turn erosion. From the additional events, S6 had marked erosion volume along the profile, which was even greater than some events captured by both CASEs. The total erosion volume of all events in CASE *u* was about 12% higher compared with CASE *H*. These emphasize that the additional events (e.g. S6) are important to investigate the beach/dune erosion. In NR, the total erosion was lower than FR, due to the cumulative change of the profile (Fig. 9). In the first event (S1), the ridge-runnel pattern was significantly flattened, and thus provided lower erosion during the subsequent events. However, if the water level raises during the subsequent events (e.g. S9) than the previous events, the avalanching and slumping processes trigger lowering of the dune front leading to severe erosion (Roelvink et al., 2009). When the dune front has been eroded and set back during the previous events, there will be no erosion at the dune though the water level increased (e.g. S14). Dissanayake et al. (2015c) showed similar results that the dune erosion decreases, when a storm event follows a high severity event.

The overall storm impact, which was analysed using the initial and final profiles during the simulation period, was fairly similar in both CASEs as well as in both scenarios (Figs. 11 and 12). In FR, the last event (S14) was same in CASE *u* and *H* (Table 5). S14 was simulated from 05.12 to 06.12.2013 using the measured initial profile on September 10, 2013. However, the simulated final profile showed a reasonable/fair agreement (*BSS* = 0.3, Van Rijn et al., 2003) with the measured final profile on December 09, 2013, and that further increased (i.e. good agreement) depending on the analysed segment (e.g. from 0.8 to 3 m: *RMSE* = 0.09 and *BSS* = 0.8, and from −1 to 5 m: *RMSE* = 0.11 and *BSS* = 0.6 in Dissanayake et al., 2015c). It should be noted, the initial profile has been measured on September 10, 2013 after a calm period, while the final profile has been measured on December 09, 2013 after a high severe storm event (S14). Accordingly, if the measured initial profile has a prominent ridge-runnel pattern and the measured final profile has a linear shape within the inter-tidal area, the simulated final profile of any severe storm event resembles the measured final profile with a good agreement (Dissanayake et al., 2015a,c). In NR, higher erosion at the lower and upper beaches, and the dune occurred by the cumulative impact of all events than S14 in FR. Formby Point experiences erosion during storm impacts, then beach recovery depending on the following calm period, and again erosion during the next event and so on (Esteves et al., 2012; Pye and Blott, 2016). Dunes typically rollover landward (i.e. erosion at seaward and accretion at landward: per. comm. with Andrew Martin in the local council). The measured final profile has experienced these processes, but the simulated final profile has experienced only erosion in both scenarios. Therefore, the impacts of storm events in CASE *u* and *H* on the beach/dune erosion are difficult to distinguish by analysing the initial and final profiles of the simulation period.

The models overestimate dune erosion by the same amount in both CASE *u* and *H*. This indicates that they have similarly captured the occurrence of extreme water levels, though the durations of storm events are different. Several elements contribute to the overestimation of dune erosion, e.g., 1) simplification of dune granulometry, 2) accuracy of measured data, 3) 1D model approach and 4) Model physics. Dunes at Formby Point consist of different level of consolidations of sand and vegetation roots (Pye and Blott, 2008), which were not implemented in the models. Resolution of boundary forcing and profile measurement might not sufficient to capture the actual variations. Depending on the storm approach, the contribution of alongshore transport to the profile

evolution increases, and that is not present in the 1D approach. Furthermore, 1D models tend to overpredict high waves (Stockdon et al., 2014). Parameterization and assumptions of the model formulations might not fully represent the natural behaviour (Kalligeris et al., 2020). However, the overall agreement between the measured and the model profiles qualified reasonable/fair, which facilitated to investigate the storm impacts from the CASE *u* and *H* events.

6. Conclusions

A two-step framework was developed to investigate the storm driven beach/dune erosion using the data of Formby Point on the Sefton coast, UK. In the first step, a statistical analysis was carried out to derive a classification of storm events (CASE) considering the variation of water levels (*TA*) and wave heights (*Hs*). The univariate response function, $X(t) = Hs(t)+TA(t)$, was analysed for the period (t) 2005–2018. Statistical properties of the probability distributions were adopted to estimate the optimised threshold (u). The established CASE for the Sefton coast (H) is based on the variation of *Hs* only. Both CASE *u* and *H* were used to identify the storm occurrence. In the second step, the storm erosion was simulated by forcing XBeach with the derived storm events within a very extreme storm period. In order to capture the possible beach/dune response, we used two scenarios of simulations, FR: fully recovered and NR: not recovered of the profile between events. The simulated storm impacts were analysed along the lower and upper beaches, and the dune.

CASE *u* identified additional storm events (35%) compared with CASE *H*. The additional events impacted at the beaches and the dune. Storm durations of the events in CASE *u* were longer than CASE *H*. Variation of the mean *Hs* and the mean *TA* during storm events indicated that the occurrence of high *TA* dominates erosion compared to high *Hs*. In FR, the initial profile had the ridge-runnel pattern, which experienced a large morphological response during each storm event, whereas NR produced low erosion due to cumulative impact. In the event-based impact, the erosion volume of CASE *u* was higher by 12% (FR) than CASE *H*. Estimation of the overall impact using the initial and final profiles showed, both CASEs result in similar erosion volumes. The post-storm profile at Formby Point has a distinct shape, particularly within the upper beach, where the ridge-runnel pattern is prominent. During severe storm impacts, the ridge-runnel pattern is flattened, and the profile is linearized. The agreement between the simulated and the measured profiles depends on the time of the profile measurement (i.e. the initial profile after a calm period and the final profile after a severe storm event) rather than the number of storm events. The hypothesized scenarios accomplished the lower end (event-based: NR, overall impact: FR) and the upper end (event-based: FR, overall impacts: NR) of the envelope of the natural profile evolution of Formby Point. More analyses are essential to validate this approach with the event-based profile measurements, though it provided better results for the available surveys compared with CASE *H*.

This study concludes, both *Hs* and *TA* are important parameters to identify the occurrence of storm events. CASE *u* was able to capture a wide range of severity events, which showed increased storm occurrence per year representing global change of extreme events. Additional storm events of CASE *u* provided marked erosion at the dune, which is not recoverable compared to the lower and upper beaches. These events need to be identified for a comprehensive interpretation of the storm erosion and to apply suitable coastal management strategies (e.g. estimating beach nourishment volume, recession and landward rolling of dune crest). CASE *u* is independent of tidal range, and also tidal phase because storm events generally span more than 6 h. The proposed two-step framework is therefore universally applicable to investigate the storm driven erosion on beach/dune systems.

Declaration of competing interest

The authors declare that they have no known competing financial interests or personal relationships that could have appeared to influence the work reported in this paper.

Acknowledgement

This study is part of the project *MoDECS* (Modification of Dune Erosion by adjacent Coastal Systems) funded by German Research Foundation (DFG) under the grant number DI 2139/2–1. Authors greatly acknowledge Andrew Martin from Sefton Metropolitan Borough Council for providing the field data. Franck Mazas from Artelia Group is acknowledged for providing the R-routine of wave transformation.

Appendix A. Supplementary data

Supplementary data to this article can be found online at https://doi.org/10.1016/j.coastaleng.2021.103939.

References

Abu-Shawiesh, M.O.A., Saghir, A., 2019. Robust confidence intervals for the population mean alternatives to the Student-t confidence interval. J. Mod. Appl. Stat. Methods 18 (1), eP2721. https://doi.org/10.22237/jmasm/1556669160.

Armaroli, C., Ciavola, P., Perini, L., Calabrese, L., Lorita, S., Valentini, A., Masina, M., 2012. Critical storm thresholds for significant morphological changes and damage along the Emilia-Romagna coastline, Italy. Geomorphology 143–144, 34–51.

Baart, F., 2013. Confidence in Coastal Forecasts. PhD Dissertation, Delft University of Technology, the Netherlands. https://repository.tudelft.nl/.

Bart, L.J.C., 2017. Long-term Modelling with XBeach: Combining Stationary and Surfbeat Model in an Integrated Approach. Delft University of Technology. Master Thesis. https://repository.tudelft.nl/.

Berard, N.A., Mulligan, R.P., Da Silva, A.M.F., Dibajnia, M., 2017. Evaluation of XBeach performance for the erosion of a laboratory sand dune. Coast Eng. 125, 70–80.

Bernardara, P., Andreewsky, M., Benoit, M., 2011. Application of regional frequency analysis to the estimation of extreme storm surges. J. Geophys. Res. 116. C02008, 1-11.

Bernardara, P., Mazas, F., Kergadallan, X., Hamm, L., 2014. A two-step framework for over-threshold modelling of environmental extremes. Nat. Hazards Earth Syst. Sci. 14, 635–647.

Bertotti, L., Cavaleri, L., Tescaro, N., 1996. Long term wave hindcast in the Adriatic Sea. Il Nuovo Cimento 19 (1), 91–108.

Brown, J.M., Souza, A.J., Wolf, J., 2010a. An 11-year validation of wave-surge modelling in the Irish Sea, using a nested POLCOMS-WAM modelling system. Ocean Model. 33, 118–128.

Brown, J.M., Souza, A.J., Wolf, J., 2010b. An investigation of recent decadal-scale storm events in the eastern Irish Sea. J. Geophys. Res. 115, C05018. https://doi.org/10.1029/2009JC005662.

Bruce, T., Muller, G., Allsop, W., Kortenhaus, A., 2009. Criteria for wave impacts at coastal structures. Proceedings Coastal Structures. https://doi.org/10.1142/9789814282024_0075, 2007.

Callaghan, D., Nielsen, P., Short, A., Ranasinghe, R., 2008. Statistical simulation of wave climate and extreme beach erosion. Coast Eng. 55, 375–390.

Callaghan, D.P., Ranasinghe, R., Roelvink, D., 2013. Probabilistic estimation of storm erosion using analytical, semi-empirical, and process based storm erosion models. Coast. Eng. 82, 64–75.

Coco, G., Senechal, N., Rejay, A., Bryan, K.R., Capo, S., Parisot, J.P., Brown, J.A., MacMahan, J.H.M., 2014. Beach response to a sequence of extreme storms. Geomorphology 204, 493–501.

Corsini, S., Inghilesi, R., Franco, L., Piscopia, R., 2004. Atlante delle onde nei mari italiani - Italian wave atlas. Agenzia per la Protezione dell'Ambiente e per i Servizi Tecnici (APAT) and University of Rome "3". http://www.ancientportsantiques.com/wp-content/uploads/Documents/ETUDESarchivees/Waves/ItalyWaveStat-Text2004.PDF.

Dissanayake, P., Brown, J., Karunarathna, H., 2014. Modelling storm-induced beach/dune evolution: Sefton coast, Liverpool Bay, UK. Mar. Geol. 357, 225–242.

Dissanayake, P., Brown, J., Karunarathna, H., 2015a. Impacts of storm chronology on the morphological changes of the Formby beach and dune system, UK. Nat. Hazards Earth Syst. Sci. 15, 1533–1543.

Dissanayake, P., Brown, J., Wisse, P., Karunarathna, H., 2015b. Comparison of storm cluster vs isolated event impacts on beach/dune morphodynamics. Estuar. Coast Shelf Sci. 164, 301–312.

Dissanayake, P., Brown, J., Wisse, P., Karunarathna, H., 2015c. Effect of storm clustering on beach/dune evolution. Mar. Geol. 370, 63–75.

Dissanayake, P., Brown, J., Sibbertsen, P., Winter, C., 2019a. Role of water level in storm impacts of a hyper-tidal coast. In: Proceedings of the Conference Costal Sediment '19. https://doi.org/10.1142/9789811204487_0109. Tampa, Florida.

Dissanayake, P., Wurpts, A., Winter, C., 2019b. Storm Classification and the Investigation of Impacts on Beach/dune. Proceeding of the conference Coastal Structures, Hannover, Germany. https://doi.org/10.18451/978-3-939230-64-9_063.

Edmondson, S.E., 2010. Dune slacks on the Sefton coast, Sefton's dynamic coast. Proceeding of the Conference on Coastal and Geomorphology, Biogeography and Management 178–187.
Esteves, L.S., Williams, J.J., Nock, A., Lymbery, G., 2009. Quantifying shoreline changes along the Sefton coast (UK) and the implications for research-informed coastal management. Journal of Coastal Research, SI 56, 602–606.
Esteves, L.S., Williams, J.J., Brown, J.M., 2011. Looking for evidence of climate change impacts in the eastern Irish Sea. Nat. Hazards Earth Syst. Sci. 11, 1641–1656.
Esteves, L.S., Brown, J.M., Williams, J.J., Lymbery, G., 2012. Quantifying threshold for significant dune erosion along the Sefton coast, northwest england. Geomorphology 143–144, 52–61.
Garnier, E., Ciavola, P., Spencer, T., Ferreira, O., Armaroli, C., McIvor, A., 2018. Historical analysis of storm events: case studies in France, England, Portugal and Italy. Coast. Eng. 134, 10–23.
Goda, Y., 2010. Random seas and design of maritime structures. In: 3rd Edition Advanced Series on Ocean Engineering, vol. 33. World Scientific.
Haigh, I.D., Nicholls, R., Wells, N., 2010. A comparison of the main methods for estimating probabilities of extreme still water levels. Coast. Eng. 57, 838–849.
Haigh, I.D., Wadey, M.P., Wahl, T., Ozsoy, O., Nicholls, R.J., Brown, J.M., Horsburgh, K., Gouldby, B., 2016. Spatial and temporal analysis of extreme sea level and storm surge events around the coastline of the UK. SCIENTIFIC DATA 3, 160107. https://doi.org/10.1038/sdata.2016.107.
Haight, F.A., 1967. Handbook of the Poisson Distribution. John Wiley & Sons, New York.
Halcrow, 2009. North west england and north wales shoreline management plan 2, appendix C: baseline processes. http://mycoastline.org/documents/AppendixC-C.4F_Seftoncoast.pdf, 40.
Hanley, M.E., Hoggart, S.P.G., Simmonds, D.J., Bichot, A., Colangelo, M.A., Bozzeda, F., Heurtefeux, H., Ondiviela, B., Ostrowski, R., Recio, M., Trude, R., Zawadzka-Kahlau, E., Thompson, R.C., 2014. Shifting sands? Coastal protection by sand banks, beaches and dunes. Coast. Eng. 87, 136–146.
Harley, M.D., Ciavola, P., 2013. Managing local coastal inundation risk using real-time forecasts and artificial dune placements. Coast Eng. 77, 77–90.
Hosking, J.R.M., Wallis, J.R., 1997. Regional Frequency Analysis. An Approach Based on L-Moments. Cambridge University Press, Cambridge. Cambridge.
Jane, R., Dalla Valle, L., Simmonds, D., Raby, A., 2016. A copula-based approach for the estimation of wave height records through spatial correlation. Coast Eng. 117, 1–18.
Kalligeris, N., Smit, P.B., Ludka, B.C., Guza, R.T., Gallien, T.W., 2020. Calibration and assessment of process-based numerical models for beach profile evolution in southern California. Cost Eng. 158, 103650.
Karunarathna, H., Brown, J., Chatzirodou, A., Dissanayake, P., Wisse, P., 2018. Multi-timescale morphological modelling of a dune-fronted sandy beach. Coast Eng. 136, 161–171.
Li, F., van Gelder, P.H.A.J.M., Ranasinghe, R., Callaghan, D.P., Jongejan, R.B., 2014. Probabilistic modelling of extreme storms along the Dutch coast. Coast Eng. 86, 1–13.
Masselink, G., Scott, T., Poate, T., Russel, P., Davidson, M., Conley, D., 2016. The extreme 2013/2014 winter storms: hydrodynamic forcing and coastal response along the southwest coast of England. Earth Surf. Process. Landforms 41, 378–391.
Mazas, F., Hamm, L., 2017. An event-based approach for extreme joint probabilities of waves and sea levels. Coast Eng. 122, 44–59.
McCall, R.T., Masselink, G., Poate, T.G., Roelvink, J.A., Almeida, L.P., 2015. Modelling the morphodynamics of gravel beaches during storms with. XBeach-G. Coast. Eng. 103, 52–66.
McMillian, A., 2011. Coastal Flood Boundary Conditions for UK Mainland and Islands 1–142. Environment Agency, 2011.
Palmer, M.R., 2010. The modification of current ellipses by stratification in the Liverpool Bay ROFI. Ocean Dynam. 60, 219–226. https://doi.org/10.1007/s10236-009-0246-x.
Parker, W.R., 1975. Sediment mobility on a multi-barred foreshore (Southwest Lancashire, UK). In: Hails, J.R., Carr, A.P. (Eds.), Nearshore Sediment Dynamics and Sedimentation. John Wiley & Sons, London, pp. 151–179.
Pender, D., Karunarathna, H., 2013. A statistical-process based approach for modelling beach profile variability. Coast Eng. 81, 19–29.
Pickands, J., 1975. Statistical influence using extreme order statistics. Ann. Stat. 3, 119–131.
Plater, A.J., Grenville, J., 2008. Liverpool bay: linking the eastern Irish sea to the Sefton coast, sefton's dynamic coast. In: Proceeding of the Conference on Coastal and Geomorphology, Biogeography and Management, pp. 41–43.
Pye, K., Blott, S.J., 2006. Coastal processes and morphological change in the dunwich-sizewell Area, Suffolk, UK. J. Coast Res. 22 (3), 453–473.
Pye, K., Blott, S.J., 2008. Decadal-scale variation in dune erosion and accretion rates: an investigation of the significance of changing storm tide frequency and magnitude on the Sefton Coast, UK. Geomorphology 102, 652–666.
Pye, K., Blott, S.J., 2016. Assessment of beach and dune erosion and accretion using LiDAR: impact if the stormy 2013-14 winter and long term trends on the Sefton Coast, UK. Geomorphology 266, 146–167.
Quartel, S., Ruessink, B.G., Kroon, A., 2007. Daily to seasonal cross-shore behaviour of quasi-persistent intertidal beach morphology. Earth Surf. Process. Landforms 32, 1293–1307.
Roelvink, J.A., 2006. Coastal morphodynamic evolution techniques. Coast Eng. 53, 277–287.
Roelvink, D., Reniers, A., van Dongeren, A., Van Thiel de Vries, J., McCall, R., Lescinski, J., 2009. Modelling storm impacts on beaches, dunes and barrier islands. Coast Eng. 56, 1133–1152.
Roelvink, D., McCall, R., Mehvar, S., Nederhoff, K., Dastgheib, A., 2018. Improving predictions of swash dynamics in XBeach: the role of groupiness and incident-band runup. Coast Eng. 134, 103–123.
Sallenger, A., 2000. Storm impact scale for barrier islands. J. Coast Res. 16 (3), 890–895.
Schlichtholz, P., 2018. Climate impacts and Arctic precursors of changing storm track activity in the Atlantic-Eurasian region. Science Reports 8, 1–19.
Šimková, T., 2017. Statistical inference based on L-moments. Statistika 97 (1), 44–58.
Smallegan, S.M., Irish, J.L., Van Dongeren, A.R., Bieman, J.P.D., 2016. Morphological response of sand barrier island with a buried sea wall during Hurricane Sandy. Coast Eng. 110, 102–110.
Soulsby, R.L., 1997. Dynamics of Marine Sands. Thomas Telford, London.
Souza, A.J., Brown, J.M., Williams, J.J., Lymbery, G., 2013. Application of an operational storm coastal impact forecasting system. Journal of Operational Oceanography 6, 23–26.
Splinter, K.D., Carley, J.T., Golshani, A., Tomlinson, R., 2014. A relationship to describe the cumulative impact of storm clusters on beach erosion. Coast Eng. 83, 49–55.
Stockdon, H.F., Thompson, D.M., Plant, N.G., Long, J.W., 2014. Evaluation of wave runup predictions from numerical and parametric models. Coast. Eng. 92, 1–11.
Van Ormondt, M., Nelson, T.R., Hapke, C.J., Roelvink, D., 2020. Morphodznamic modelling of the wilderness breach, Fire Island, New York. Part I: model set-up and validation. Coast. Eng. 157, 103621.
Van Rijn, L.C., 2007. Unified view of sediment transport by currents and waves: part l and ll. J. Hydraul. Eng. 649–667.
Van Rijn, L.C., Walstra, D.J.R., Grasmeijer, B., Sutherland, J., Pan, S., Sierra, J.P., 2003. The predictability of crossshore evolution of sandy beaches at the scale of storm and seasons using process-based profile models. Coast Eng. 47, 295–327.
Vousdoukas, M.I., Ranasinghe, R., Mentaschi, L., Plomaritis, T.A., Athanasiou, P., Luijendijk, A., Feyen, L., 2020. Sand Coastlines under Threat of Erosion, Nat. Climate Cha, vol. 10, pp. 260–263.
Wolf, J., Brown, J.M., Howarth, M.J., 2011. The wave climate of Liverpool Bay – observations and modelling. Ocean Dynam. 61, 639–655.